

ORNL CF 60-7-46

UNIT OPERATIONS SECTION MONTHLY PROGRESS REPORT

July 1960

CHEMICAL TECHNOLOGY DIVISION

M. E. Whatley

P. A. Haas

R. W. Horton

A. D. Ryon

J. C. Suddath

C. D. Watson

Date Issued

OCT 27 1960

OAK RIDGE NATIONAL LABORATORY
Oak Ridge, Tennessee
Operated By
UNION CARBIDE CORPORATION
for the
U. S. Atomic Energy Commission

DISCLAIMER

This report was prepared as an account of work sponsored by an agency of the United States Government. Neither the United States Government nor any agency Thereof, nor any of their employees, makes any warranty, express or implied, or assumes any legal liability or responsibility for the accuracy, completeness, or usefulness of any information, apparatus, product, or process disclosed, or represents that its use would not infringe privately owned rights. Reference herein to any specific commercial product, process, or service by trade name, trademark, manufacturer, or otherwise does not necessarily constitute or imply its endorsement, recommendation, or favoring by the United States Government or any agency thereof. The views and opinions of authors expressed herein do not necessarily state or reflect those of the United States Government or any agency thereof.

DISCLAIMER

Portions of this document may be illegible in electronic image products. Images are produced from the best available original document.

ABSTRACT

A critical review of the literature revealed no experiments on uranyl ion transfer from an aqueous to a tributyl phosphate phase which positively measured the kinetics of the chemical reaction at the interphase. Drawing isorithmic lines on a three component diagram gives a complex correlation for the compaction of three sizes of glass beads. Neither the use of thorium sols nor high feed solution concentrations of thorium nitrate gave any significant increase in mean particle diameters over those obtained from nitrate solutions of lower concentrations in flame denitration. A hydraulic film resistance has been detected in the anion exchange of uranyl sulfate into Dowex 21K and chloride elution was found to give a higher apparent uranium diffusion coefficient than nitrate elution. The rate of dissolution of mixed thorium-uranium oxides was determined as a function of the per cent of mixed oxides dissolved. Mixing in tanks packed with boron glass raschig rings is being continued. The SRE hydraulic dejacketer has been operated successfully with prototype fuel rods. Excessive foaming was encountered when sheared stainless clad UO_2 was suddenly contacted with boiling 13 M nitric acid. While attempting to shear a prototype Yankee subassembly with Kanigan brazed diffusion bonded joints, a five tube aggregate was formed at one of the two ferrule locations sheared. Of the 91 protective coatings exposed to ionizing radiation from the HRE, 25 of the coatings outside of the shield and 10 coatings inside the shield exhibited satisfactory resistance. HETS values in the acid Thorex flowsheet are reported. Waste calcination of simulated Purex waste in a 7-in.-dia vessel gave rates slightly higher than predicted by the radial deposition model because of loss of feed due to excess foaming.

CONTENTS

	<u>Page</u>
Abstract	2
Previous Reports in This Series for the Year 1960	4
Summary	5
1.0 Chemical Engineering Research	8
2.0 Fuel Cycle Development	15
3.0 HR Fuel and Blanket Studies	17
4.0 GCR Coolant Cleanup	18
5.0 Ion Exchange	21
6.0 Power Reactor Fuel Processing	26
7.0 Solvent Extraction Studies	43
8.0 Volatility	58
9.0 Waste Processing	65

Previous Reports in this Series for the Year 1960

January	ORNL CF 60-1-49
February	ORNL CF 60-2-56
March	ORNL CF 60-3-61
April	ORNL CF 60-4-37
May	ORNL CF 60-5-58
June	ORNL CF 60-6-11

All previous reports in this series are listed in the June 1960 report, CF 60-6-11, from the beginning, December 1954.

SUMMARY

1.0 CHEMICAL ENGINEERING RESEARCH

A critical review was made of the literature in which interfacial resistances or studies of transfer of uranyl ion across the water-tributyl phosphate interface were reported. It was found that, with one or two notable exceptions, all interfacial resistances reported could be accounted for in terms of diffusion or hydrodynamic phenomena. No experiments on uranyl ion transfer had positively measured the kinetics of the chemical reaction at the interface, due to its speed.

2.0 FUEL CYCLE DEVELOPMENT

Re-examination of data using glass beads to study the effects of size distribution shows a complex correlation for three fractions obtained by drawing isorithmic or constant density lines on a three component diagram.

3.0 HR FUEL AND BLANKET STUDIES

Neither use of thoria sols as feeds nor increase of the feed solution concentrations to 1226 g/liter of $\text{Th}(\text{NO}_3)_4$ gave any significant increase in mean particle diameters over those obtained for nitrate solutions of lower concentrations, in flame denitration.

4.0 GCR COOLANT CLEANUP

A kinetics study has been started on a platinum catalyst for the oxidation of H_2 , CO and CH_4 with O_2 in helium.

The literature survey of light scattering particle detectors was completed and a preliminary design is in progress.

5.0 ION EXCHANGE

Three runs with 960 μ Dowex 21K at flow rates greater than 13 cm/sec gave a uranium self-diffusion coefficient of 2.6×10^{-8} cm²/sec. Equivalent runs with 1200 μ resin gave a coefficient of 4.4×10^{-8} cm²/sec. A run made with a flow rate of 6 cm/sec showed signs of significant film resistance. A chloride elution run with 1200 μ resin gave an apparent uranium diffusion coefficient of 2.38×10^{-7} cm²/sec which was somewhat higher than the corresponding value (1.8×10^{-7}) for nitrate elution.

6.0 POWER REACTOR FUEL PROCESSING

6.1 Darex-Thorex

The rate of dissolution of $\text{ThO}_2\text{-UO}_2$ in 13 M HNO_3 --0.04 M NaF --0.1 M $\text{Al}(\text{NO}_3)_3$ was determined as a function of per cent of mixed oxide dissolution; results were as follows:

% ThO ₂ -UO ₂ dissolution	0	1	60	80
Rate, mg/g x min	0.32	0.56	~1.0	~2.0

Sharp changes in rate were noted between 0 and 1% and at 80% dissolution.

6.2 Evaluation of Packed Process Tanks

Use of high-boron glass packing in conventional tanks as a method of criticality control is being planned. Tests were made to determine whether mixing characteristics were adversely affected by the presence of the packing. An electrical conductivity probe used in situ indicated that complete mixing time for solution in a tank packed with 1-1/2-in.-dia x 1-3/4-in. glass raschig rings varied inversely as the solution volume. Results at an air rate of 0.5 scfm/ft² to the peripheral sparge ring were 23 min for 85 gal, 7 min for 150 gal.

6.3 Mechanical Processing

SRE De jacketing Studies. The hydraulic de jacketing unit operated satisfactorily in processing prototype fuel rods (containing steel slugs and no NaK) through each sequence of operation of: (1) cutting through the clad to remove the end caps, (2) expanding the jackets, (3) ejecting the slugs, and (4) winding the empty jacket into a spiral roll for disposal.

Leaching. Excessive foaming occurred when the sheared fines from 7.5 kg stainless clad UO₂ were suddenly contacted with boiling 13 M HNO₃. Sudden immersion of sheared UO₂ fines in boiling concentrated HNO₃ is indicated as not being feasible. At the end of this run 12 g (0.16% of 7.5 kg charge) flocculent residue (tap density 0.44) repeatedly plugged a 0.5-in.-dia tubing outlet while the uranyl nitrate product was being drained (at 50°C).

Shearing. Tests on tubular bundles of metal-clad, ceramic fuel pellets showed that the physical properties of the bond metal used to form ferrule-to-tube joints had a great influence on whether single, discrete pieces or clumps of tube sections were produced when shearing at ferrule locations. A 3 ft long section of a stainless steel, porcelain-filled Yankee prototype subassembly (36 - 0.337-in.-dia tubes) assembled with diffusion-bonded, Kanigan-brazed ferrule-to-tube joints was sheared at 1-in. intervals using an "M" shaped punch and 90° anvil. At one of two ferrule locations sheared, five 2-tube pieces and one 5-tube piece remained integral. The largest section produced on shearing a Mark I prototype (36 - 0.5-in.-dia tubes), brazed with more brittle Microbraz 50, was one 2-tube piece. Large multi-tube agglomerates incompatible with continuous processing were produced on shearing a Mark I prototype assembly by ferrule-to-tube welds. This construction was made to simulate the ultimate that might be approached in further development of a strong, ductile, braze alloy for use in assemblies multi-tube fuel elements.

A concept of chop-leach equipment incorporating a simplified method of solid material transfer is presented.

Cost Study. A preliminary cost study has been initiated to evaluate the relative economics of fuel processing by a chop and leach technique versus aqueous decladding of stainless steel clad, ceramic fuels. The cost study will be used to evaluate the ultimate usefulness of the chop-leach concept in fuel processing and as an aid in directing the emphasis of subsequent development programs.

6.4 Radiation Damage Studies

Ninety-one protective coatings were exposed to ionizing radiation from both inside and outside of the thermal shield during 9,030 hours of operation of the HRE. Initial observations indicate that 25 of the coatings outside of the shield and 10 of the coatings inside the thermal shield exhibited satisfactory resistance to both radiation and water.

7.0 SOLVENT EXTRACTION STUDIES

In studies of the stage efficiency of pulse columns as a function of cartridge design with the acid Thorex flowsheet, the HETS values for thorium extraction in a sieve plate column (0.125-in.-dia holes, 23% free area) were 2.1 ft for aqueous-continuous (top interfaces) and 4.0 ft for organic-continuous (bottom interface) operation. The HETS values in a nozzle plate column operated organic-continuous were 4.0 ft for the large nozzle cartridge (0.188-in.-dia nozzle, 23% free area) and 3.0 ft for the small nozzle cartridge (0.125-in.-dia nozzle, 10% free area). All experiments were conducted with a pulse frequency of 50 cpm and an amplitude of 1 in.

8.0 VOLATILITY

The procedures for determining the dissociation pressure of various fission product fluoride - sodium fluoride complexes are described and discussed. An initial effort to prepare MoF_6 is reported.

9.0 WASTE PROCESSING

In a calcination run with simulated Purex waste in a 7-in.-dia vessel, the processing rate averaged over the feeding period to fill 90% of the vessel was 25.6 liters/hr. According to the radial deposition model, the rate should have been 20 liters/hr, as it was in previous runs with 6 and 8-in.-dia vessels. The discrepancy was caused by excessive foaming, which carried liquid feed into the condensate.

Of the non-radioactive ruthenium added to the liquid feed, 16% remained in the calcined solids, 25% was found in the condensate, and 59% was unaccounted for.

An apparatus is being built for studying the growth of soluble aerosols in a wetted wall tower.

1.0 CHEMICAL ENGINEERING RESEARCH

A. D. Ryon

1.1 Resistance to Mass Transfer at a Fluid Interface - C. V. Chester

Evidence for a Chemisorbtion--or Membrane--Type Resistance at a Fluid Interface. Various investigators have, from time to time, reported interfacial resistances, or effects attributable to interfacial resistance, which cannot be explained by hydrodynamic effects.

One of the earliest observations of such resistance was reported by Higbie⁶ in 1935, who observed that K_L for the absorbtion of CO_2 in water did not go to infinity as the time of contact went to zero. His observations can be accounted for by a resistance at the interface equivalent approximately to that of a 10 micron layer of water at steady state.

It might be injected parenthetically here that resistances will be discussed in terms of an equivalent film of water or other pertinent solvent in order to give a physical feeling for the order of magnitude of the effects considered. The qualification of steady state transfer must be added to the analogy as the "film" has no capacity for the solute.

Higbie's evidence for the resistance is quite indirect, requiring extrapolation of the experimental data. It has been subject to considerable question, and has been difficult to reproduce.

In 1959 E. A. Harvey⁵ reported a study of the same system with transfer across a quiescent interface, using an extraordinarily sensitive interferometric technique. In his experiments the penetration of CO_2 into a plane, quiescent interface in a cell was followed by observation of the displacement of interference fringes caused by change in the refractive index of the solution with CO_2 concentration. There was no resistance observed when pure water was exposed to a pure CO_2 atmosphere. The sensitivity claimed for the technique is an interfacial rate constant as large as 4 cm/sec which corresponds to a steady state film resistance of less than 0.1 micron.

When a surface active agent (0.41% "lissapol-N") was introduced to the aqueous phase, the rate constant was 0.028 cm/sec which corresponds to a film of about 10 microns. This is one of the very few experiments where there is clear evidence that a surface active agent produced a "membrane-type" resistance to mass transfer. However, it should be pointed out that the bulk solubility of the agent is zero in the gas phase, and one might expect somewhat different behavior of a gas liquid interface than that between two liquids.

In 1952 Tung and Drickamer¹⁴ reported studies of the diffusion of tagged sulfur compounds through a liquid-liquid interface in which very large interfacial resistances were observed. The experiments were carried out in a diffusion cell designed for high-pressure work using an unsteady state technique. In an experiment, some of the diffusing compound tagged with sulfur-35 was introduced at one end of a wire-gauze-packed diffusion path, and the output of a beta detector at the other end of the path was observed as a

function of time. The equivalent diffusion path length was determined by calibration with a solute of known diffusivity (sulfuric acid). The diffusivity of an unknown solute could then be calculated from the path length, concentration buildup of the tagged solute, and the equations for diffusion in one dimension. In this manner diffusion coefficients were measured for SO₂ in liquid SO₂ and in n-heptane, and for sulfuric acid in phenol. The experiment was repeated for SO₂ with the cell half full of liquid SO₂ and filled the rest of the way with n-heptane in such a manner that the interface was normal to the direction of diffusion. The relaxation time for the concentrated profile in the cell was much longer with the two phases than with either single phase. Or, to state it another way, the apparent diffusion coefficient was much less in two phases than in either single phase. This was interpreted to mean that there was a large interfacial resistance to diffusion. This resistance comes out to be equivalent to a steady state film on the order of centimeters thick.

The same phenomenon was observed for the case of diffusion of sulfuric acid through phenol and water. A marked decrease in apparent diffusion coefficient was observed when the diffusion sulfuric acid had to cross the water-phenol interface. This decrease corresponded to an interfacial resistance on the order of centimeters of solvent. These experiments showed the largest resistances reported for liquid-liquid interfaces in the literature. There are no obvious weaknesses in technique or interpretation of data, but no one has produced similar results in the same or chemically similar systems. This uniqueness of the findings after some years' elapse might lead one to question them.

Explanation of the existence of an interfacial resistance, and in particular, in the systems mentioned above, was attempted by Sinfelt and Drickamer¹³ in 1955. They liken the slow reaction at the interface to a chemisorbtion process, having a high energy of activation.

Other studies of interfacial resistance have grown out of the biological work on transfer of solutes through a cell wall. In 1948 Hutchinson⁷ studied the transfer of alcohols between water and benzene with the possibility of a monomolecular detergent film present. Unfortunately his experiments were of a crude stirred interface type, with diffusion and Marengoni effects ignored. It was found that the detergent film retarded the transfer, but this could easily have been due to hydrodynamic effects.

In 1949 J. T. Davies³ presented a study of the transfer of salts from water to benzene in a stirred-interface equipment. The experimental work was carefully carried out, but there is a gross flaw in the analysis due to the implicit assumption that all the resistance to transfer was in the interface, and that diffusion in the bulk phases could be ignored. It was observed that rate of stirring had an effect on diffusion time, so the author made the incredible decision to correct all his data to zero stirrer speed. The correction factor was only 0.58, i.e., the relaxation time for 100 rpm was 0.58 that for no stirring, indicating the very low efficiency of stirring.

about the same for extraction and stripping, and only slightly less than the normal stripping coefficient. It will be recalled that uranyl extraction is quite exothermic, and hence would be expected to produce considerable Marengoni turbulence and be correspondingly sensitive to interfacial viscosity.

Although useless for design purposes, Burgher's work is valuable for the many qualitative observations made on the behavior of the uranyl-TBP system. The general behavior with surface active agents, and coalescence observations are important and generally can be explained in terms of interfacial tension and viscosity changes. The need for extensive work on the hydrodynamics of the water-TBP interface during uranyl transfer is best shown by this work.

The fixed-interface, stirred-bulk experiments that have come closest to the ideal of eliminating diffusion resistance in the bulk were those reported by Keish⁸ in 1959. His apparatus consisted of a half-inch-diameter cylindrical chamber about an inch deep containing a coaxial 1/8-in. stirring shaft. A sharp constriction in the chamber at the interface reduced the specific interfacial area of the system to permit reasonable run times and also to prevent (it is hoped) longitudinal motion or "pumping" of the interface. He studied isotope exchange, with the phases at gross chemical equilibrium, and thereby eliminated all the problems associated with Marengoni turbulence.

The data taken were analyzed in terms of the isotope exchange law as given by Wahl and Bonner. In this law, the rate of exchange is equal to a product of two factors, one containing essentially the distribution coefficient, the other a rate term. The calculated exchange rate shows the same variation with various ion concentrations as the distribution coefficient, but the rate term is remarkably constant.

The fact that the system relaxed to equilibrium (of the uranium isotope distribution) with such remarkably constant half life for all the changes in concentration strongly suggests a diffusion controlled process, rather than the kinetic one postulated by the author. However, assuming diffusion control in a film, the calculated film thickness is on the order of 0.25μ , which is by far the thinnest film or equivalent film yet observed. It is possible that the interfacial area (0.04 cm^2) was not as well defined as assumed, as it is possible that some vertical perturbations might have occurred, which would greatly increase interfacial area, and correspondingly decrease equivalent film thickness calculated on the basis of ideal area.

The actual case in Keish's experiments is quite likely a combination of diffusion and chemical kinetic control. The experiments show that the reaction is very fast indeed, and not at all limiting in engineering mass-transfer operations.

Conclusions. From this review of mass-transfer experiments, with emphasis in the Uranium-TBP system, a few observations and generalizations can be drawn:

1. Fixed-interface, stirred-bulk experiments are of questionable value for obtaining quantitative data on mass transfer in any system where the transfer reactions are as fast in the U-TBP system. These experiments are useful for making qualitative or comparative observations or for scouting experiments.

2. To eliminate all questions concerning interfacial area and interfacial concentration, such as arise in stirred experiments, the area and concentration profile should be under direct optical observation during some experiments at some stage of the experimental program.

3. By far the most sensitive technique for observing concentration changes during diffusion is that based on interferometry making use of the change of index of refraction of solutions with concentration.

4. Any subsequent work on the U-TBP interfacial chemical kinetics should use an interferometric technique similar to that of Harvey⁵ using phases with small concentration differences from equilibrium. Resistances to transfer as small as a few hundred angstroms of solution could be detected, and separated completely and positively from transport effects.

5. The hydrodynamic behavior of the interface is a separate problem, and should be recognized as such, and treated separately. Since transport to the interface is rate limiting in engineering operations, and this is most strongly affected by the interfacial hydrodynamics, it is to this problem that engineering research should be addressed.

Bibliography.

1. Burger, L. L., "The Transfer of Uranyl Nitrate Across the Water-Tributyl Phosphate Interface," HW-62087 (1959).
2. Chester, C. V., "Transfer of Uranyl Ion Across a Water-TBP Interface," ORNL CF 60-3-119 (1960).
3. Davies, J. T., "The Mechanism of Diffusion of Ions Across a Phase Boundary and Through Cell Walls," J. Phys. Colloid Chem. 54, 185 (1950).
4. Hahn, H. T., "The Mechanism of Uranium Extraction by Tributyl Phosphate," HW-32626 (1954).
5. Harvey, E. A. and W. Smith, "The Absorbtion of Carbon Dioxide by a Quiescent Liquid," Chem. Eng. Sci. 10, 274 (1959).
6. Higbie, R., "The Rate of Absorbtion of a Pure Gas into a Still Liquid During Short Periods of Exposure," Trans. A. I. Chem. Eng. 31, 365 (1935).
7. Hutchinson, E., "Diffusion Across Oil-Water Interfaces," J. Phys. Colloid Chem. 52, 897 (1948).
8. Keisch, Bernard, "Exchange Studies of the Uranium-Tributyl Phosphate Reaction," IDO-14490 (1959).

9. Lewis, J. B., "The Mechanism of Mass Transfer Across Liquid-Liquid Interfaces. Part I: The Determination of Individual Transfer Coefficients for Binary Systems," Chem. Eng. Sci. 3, 248 (1954).
10. Lewis, J. B., "The Mechanism of Mass Transfer of Solutes Across Liquid-Liquid Interfaces. Part II: The Transfer of Organic Solutes Between Solvent and Aqueous Phases," Chem. Eng. Sci. 3, 260 (1954).
11. Lewis, J. B., "The Mechanism of Mass Transfer of Solutes Across Liquid-Liquid Interfaces. Part III: The Transfer of Uranium Between Solvent and Aqueous Phases," Chem. Eng. Sci. 8, 295, June 1958.
12. Sherwood, T. R., "The Mechanism of Mass Transfer of Solutes Across Liquid-Liquid Interfaces," Chem. Eng. Sci. 4, 290 (1955).
13. Sinfelt, J. H. and H. G. Drickamer, "Resistance in a Liquid-Liquid Interface. Part III: The Effect of Molecular Properties," J. Chem. Phys. 23, 1095 (1955).
14. Tung, L. H. and H. G. Drickamer, "Diffusion Through an Interface - Binary System" J. Chem. Phys. 20, 6, 10 (1952).

2.0 FUEL CYCLE DEVELOPMENT

P. A. Haas

Studies are being conducted on fuel element fabrication procedures economically adaptable to remote operation for recycle of the fissile and fertile materials used in power reactors. The initial emphasis is on vibratory compaction of high density particles of ThO_2 or $\text{ThO}_2\text{-UO}_2$ of controlled size distributions. This has included studies of the compaction of arc-fused ThO_2 and $\text{ThO}_2\text{-UO}_2$ by both pneumatic and electronic vibrators and preliminary consideration of chemical methods of densifying ThO_2 .

2.1 The Effect of Particle Size Distribution on Vibratory Compaction - J. W. Snider, S. D. Clinton

A three phase diagram for the following glass bead fractions, coarse fraction No. 4, medium fraction No. 15, and fine fraction No. 20, was completed in the region of highest density (see January 1960 Unit Operations monthly progress report, CF 60-1-49, for individual bead fraction size distributions). The isorithm lines (lines of constant density) shown on Figure 2.1 are tap densities obtained in a 100 ml graduate.

The isorithmic lines reveal a more complex density-composition relationship than was expected. If the fine fraction is held constant at 13.5 wt % and a small increase of 1.5 wt % coarse fraction from 67 wt % to 68.5 wt % is made the density decreases from ~2 g/cc to 1.92 g/cc. Such sensitivity to small composition changes was unexpected. If the coarse fraction is held constant at a value between 67.5 wt % and 72.5 wt %, and the medium fraction increased from zero wt % the density will first increase pass through a maxima then through a minima and through a second maxima. The presence of this gully (considering density plotted in the third dimension) was also unexpected.

The shaded area shown on Figure 2.1 is an area of doubtful validity at the present time. The isorithm at 2.00 g/cc may extend into this area and envelope it, or an isolated isorithm may exist. Additional data will be obtained after a new supply of glass beads is received.

UNCLASSIFIED
ORNL-LR-DWG 51319

Legend: Isorithmic lines of constant densities in g/cc ● are points of 2.00 g/cc

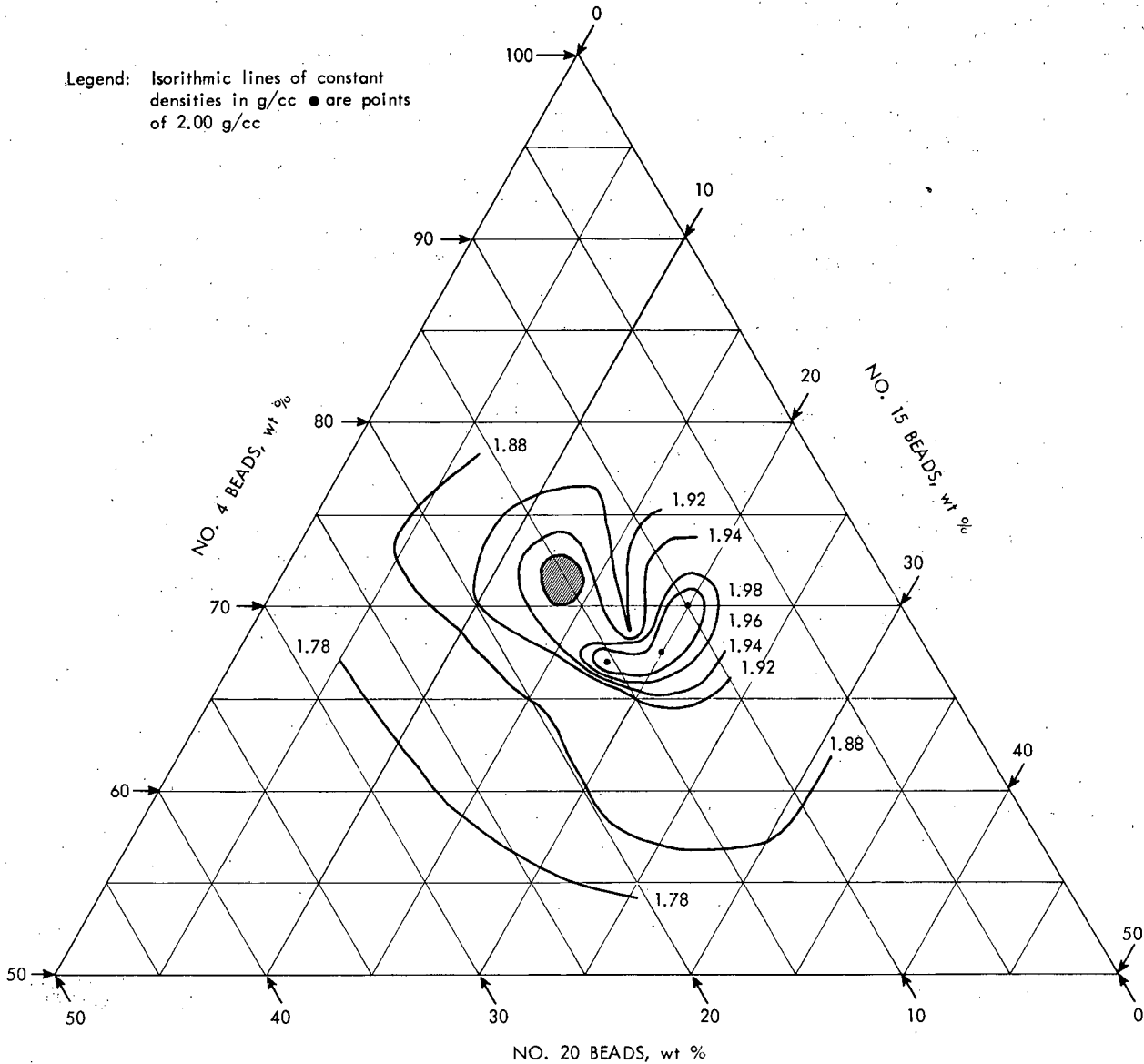


Fig. 2.1. A three-phase diagram of a three-component glass bead system with isorithmic lines.

3.0 HR FUEL AND BLANKET STUDIES

P. A. Haas

These studies are intended to develop processing and preparation methods as required for aqueous homogeneous reactor fuel and blanket fluids. The operation of a number of hydroclones in parallel on one induced underflow receiver is being studied to obtain information for interpreting results with the HRT multiclone. Flame calcination studies are directed toward obtaining 5 to 10 μ dia thoria-alumina particles with the properties previously obtained for 1 to 2 μ dia material.

3.1 Flame Calcination - C. C. Haws, Jr., V. L. Fowler

Two sol firings were made at the reference temperatures of 1000 and 1500°C with the objective of obtaining 5 to 10 μ mean dia product particles. The particles obtained in these firings were the same size as those from previous reference runs (Table 3.1). Apparently the amount of gas liberated during the drying and calcination does not control the product particle size.

The postulated subdivision of the fuel droplets and/or solids formed from these droplets has been discussed in previous reports on this work. This explosive subdivision could result from gases entrapped within the particles and/or thermal shock. It was reasoned that a thoria sol, which is essentially free of the nitrate radical, would experience less internal gas liberation. The degree of subdivision with a sol feed might then be less, and thus larger particles obtained.

The effect of very high feed concentrations at the reference temperature of 1500°C was tested. There was no appreciable effect on the product particle size (Table 3.1).

The conclusion reached from the above and other previous tests is that the particle size is temperature (rate of heat transfer to and within the particle) controlled for reflector temperatures above 1000°C.

Table 3.1. Characteristics of Flame Calcined Products Using Thoria Sols and High Concentration Nitrate Solutions as Feed Materials

Run No.	Temp. °C	Feed Description ^a		Surface Area sq m/g	Avg. Part. Size micron
		Composition	Concentration g/liter		
104	1500	ThO ₂ Sol	264	0.94	1.8
105	1000	ThO ₂ Sol	280	3.2	2.5
106	1500	ThNT ^b	920	1.3	1.8
107	1450	ThNT ^b	1226	1.7	2.0

^aAll feeds contained 5 wt % Al₂O₃ equivalent based upon total oxide weight in product.

^bWater used as solvent.

4.0 GCR COOLANT CLEANUP

J. C. Suddath

The object of this program is to obtain experimental data for the design of optimum GCR coolant purification systems for high temperature, gas-cooled power reactors. The coolants being considered are CO₂, He, and H₂ with both radioactive and non-radioactive contaminants. Immediate emphasis is being placed on contaminants in helium.

4.1 Particle Detection by Light Scattering - J. C. Suddath

Fission products released from the fuel elements cooled by helium are expected to nucleate in the gas stream forming particulate material that can be physically removed from the gas stream. In order to better predict the behavior of the particulate material and design methods for their collection, a device for measuring the concentration and size distribution in the gas stream is being designed. The device will measure the scattered light from particulates.

4.2 Evaluation of Girdler G-43 Platinum Catalyst - C. D. Scott

In the helium purification system for the EGCR recommended by Anderson,¹ oxidation of H₂, CO, and hydrocarbons was to be accomplished by oxygen addition to the purification stream followed by catalytic oxidation. The catalyst recommended was Girdler type G-43 platinum catalyst. Personnel in the Reactor Projects Division are currently testing a small scale model of the EGCR purification system which was recommended by Anderson. These tests are for purposes of component testing and do not include reaction kinetic tests as such with the G-43 catalyst.

The Technical Service Department of Chemical Products Division of Chemetron Corporation (manufacturers of Girdler Catalyst G-43) were contacted for possible experimental information on the kinetics of the oxidation of H₂, CO, and hydrocarbons with their type G-43 catalyst.² Since this catalyst had been developed for a different application, they had no information on this specific problem. However, they felt that the information available on reduction of oxides of nitrogen with hydrogen and carbon monoxide indicated that the G-43 catalyst would be suitable for our application. They recommended a bed temperature of greater than 800°F and gas space velocities in the range of 1,000 to 20,000 scfh gas/cubic foot of catalyst.

In order to back up the work of Reactor Projects Division and to give design data with more general application a short kinetics study has been started on the platinum catalyst for oxidation of H₂, CO, and CH₄. This study will be done with the available equipment in the GCR Coolant Purification Test Facility (May Unit Operations monthly progress report). To expedite the study a limited range of parameters will be investigated. Contaminant concentrations of approximately 1.0% and 0.5% will be used at a bed temperature of 500°C and at 300 psia. Total gas flow rates of approximately 28 and 90 slpm will be used.

Physical Properties of G-43 Catalyst. The G-43 catalyst is in the form of solid cylindrical tablets with nominal dimensions of 1/4-in. x 1/4-in. The bulk density of the catalyst is approximately 0.95 g/cc and the average specific surface area of two samples was 178 m²/g.

Experimental Procedure. Several tests have been made with a fixed bed of the G-43 catalysts in the 2-in.-dia oxidizer in the GCR Coolant Purification Test Facility. The oxidizer was initially charged with a known amount of catalyst. After the charged oxidizer was heated to 500°C, a preheated stream of pure helium was introduced to the oxidizer and the catalyst bed was allowed to reach thermal equilibrium at an average temperature of 500°C + 10°C. Hydrogen was introduced to the helium stream at a constant rate prior to the gas preheaters and oxygen was introduced to the total gas mixture immediately prior to its entry to the oxidizer. (Oxygen addition at this point was necessary to prevent pre-reaction of the hydrogen and oxygen in the gas preheaters due to the catalytic action of the walls of the heating coils.) The oxygen content of the helium stream was varied from slightly greater than the stoichiometric amount where there was no hydrogen in the oxidizer off-gas to a value less than the stoichiometric amount at which there was no oxygen in the off-gas.

The hydrogen and oxygen content of the off-gas was measured by a gas absorption chromatograph which had a lower limit of detection for hydrogen of approximately 20 ppm by volume and for oxygen of less than 5 ppm.

Experimental Results. A series of four runs was made with initial hydrogen concentrations of 0.40 to 2.08% with catalyst bed depths of 1-in. and 6-in. in the 2-in.-dia oxidizer. The average bed temperature was 500°C + 20°C with variations in the bed temperature in the 6-in. bed of + 50°C. Oxygen content of the gas stream varied from 18% greater than the stoichiometric amount to 41% less than the stoichiometric amount (Table 4.1) and the total gas flow rate was from 28.2 slpm to 28.7 slpm.

Correlation of Data. No attempt has been made to correlate the experimental data as yet. However, the general approach will be to determine an apparent reaction rate as a function of the mass flow rate of the gas and the partial pressures of oxygen and hydrogen. Such a correlation as outlined by S. Weller³ will not establish rate controlling mechanism of the reactions but it is adequate for design purposes. After the apparent reaction rate has been established by the above method it can be used in the reactor design equation as described in the May 1960 Unit Operations monthly progress report.

References.

1. Anderson, F. A., "Proposed Helium Purification System for the Experimental Gas-Cooled Reactor (EGCR)," ORNL-1959.
2. Personal communications with Mr. Allan of the Technical Service Department of Chemical Products Division of Chemetron Corporation, Louisville, Kentucky on July 20, 1960.
3. Weller, Sol, "Analysis of Kinetic Data for Heterogeneous Reactions," A.I.Ch.E. Journal, Vol. 2, No. 1, p. 39 (1956).

Table 4.1. Experimental Results of Platinum Catalyst Evaluation Runs

Run No.	Catalyst Bed height, in.	Total gas flow rate slpm	Average Bed Temperature °C	Initial Concentration Volume %		Reaction, % of Initial	
				H ₂	O ₂	H ₂	O ₂
3A	1.0	28.7	520	2.08	1.00	90.5	94.1
3B	1.0	28.7	500	2.08	0.80	73.4	95.2
3C	1.0	28.7	515	2.08	0.59	54.8	96.7
4A	6.0	28.7	515	2.00	1.02	100.0	98.0
4B	6.0	28.7	510	2.00	0.97	94.6	97.5
4C	6.0	28.7	490	2.00	0.91	90.0	99.0
4D	6.0	28.7	500	2.00	0.89	88.3	99.4
4E	6.0	28.7	515	2.00	0.72	72.0	99.7
4F	6.0	28.7	490	2.00	0.68	67.8	99.6
5A	6.0	28.4	505	1.00	0.42	84.0	100.0
5B	6.0	28.4	495	1.00	0.49	98.1	99.8
5C	6.0	28.4	480	1.00	0.50	98.6	98.6
5D	6.0	28.4	480	1.00	0.51	98.8	97.8
5E	6.0	28.4	490	1.00	0.53	99.8	94.2
6A	6.0	28.2	480	0.40	0.29	100.0	69.0
6B	6.0	28.2	510	0.40	0.26	99.4	76.4
6C	6.0	28.2	490	0.40	0.25	99.1	79.3
6D	6.0	28.2	490	0.40	0.19	95.0	100.0

5.0 ION EXCHANGE

J. C. Suddath

To make rational predictions of the operating characteristics of uranium anion exchange contactors, an understanding of the mechanism and kinetics of the exchange is necessary. Toward this objective the equilibrium sorption isotherms and rates of sorption of uranium on Dowex 21K are being determined.

5.1 Uranium Anion Exchange Kinetics Studies - J. S. Watson

Studies of uranyl sulfate self-diffusion in Dowex 21K have continued. The self-diffusion coefficient has been determined for 960 μ resin. Four runs were made with solution flow rates of 6, 13, 17 and 19 cm/sec (ml/sec-cm²). Although the data was badly scattered the last three runs gave essentially identical values for the average self-diffusion coefficient (approximately 2.60×10^{-8} cm²/sec) indicating that particle diffusion is the rate controlling mass transfer step under the higher solution flow rates. The results of these runs are shown in Figures 5.1, 5.2, and 5.3. The coefficient was notably lower than had been observed with 1200 μ resin. This was expected because a similar behavior has been observed during other ion exchange processes in different size fractions of Dowex 21K. The run made with a solution flow rate of 6 cm/sec gave indications that film diffusion was significant under those conditions (Figure 5.4). The loading curve lay below those observed with higher flow rates and did not have the shape predicted by particle diffusion.

A chloride elution run was made using 1200 μ Dowex 21K equilibrated with a 0.006 M uranyl sulfate solution 0.026 M in total sulfate. The eluting solution was 1 M sodium chloride. The results are shown in Figure 5.4. They may be approximated by the curve corresponding to an apparent uranium diffusion coefficient of approximately 2.38×10^{-7} cm²/sec. This value is slightly higher than was obtained for nitrate elution of the same resin (1.8×10^{-7} cm²/sec).

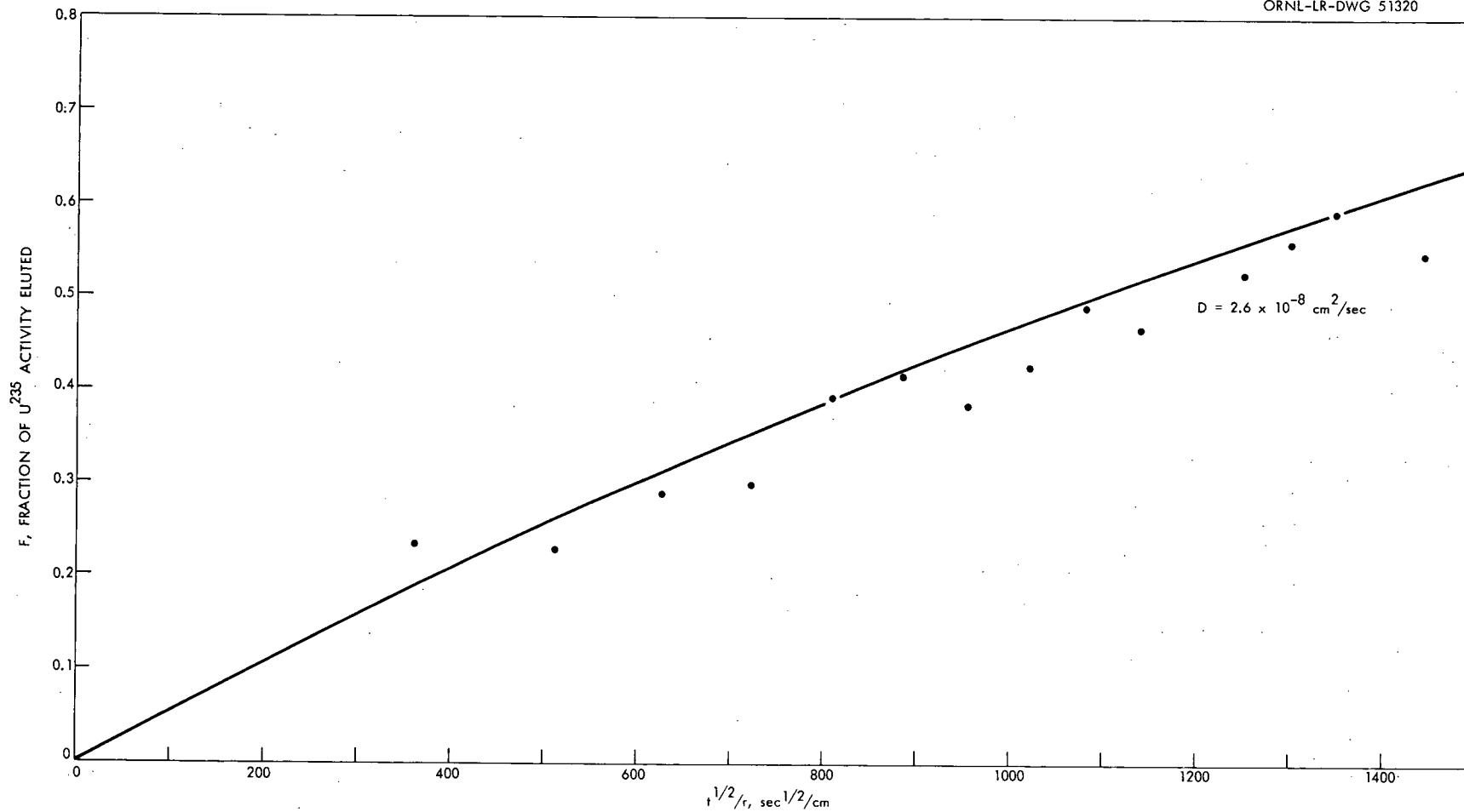


Fig. 5.1. Self-diffusion of uranyl sulfate in 960 μ Dowex 21 K with a solution flow rate of .13 cm/sec.

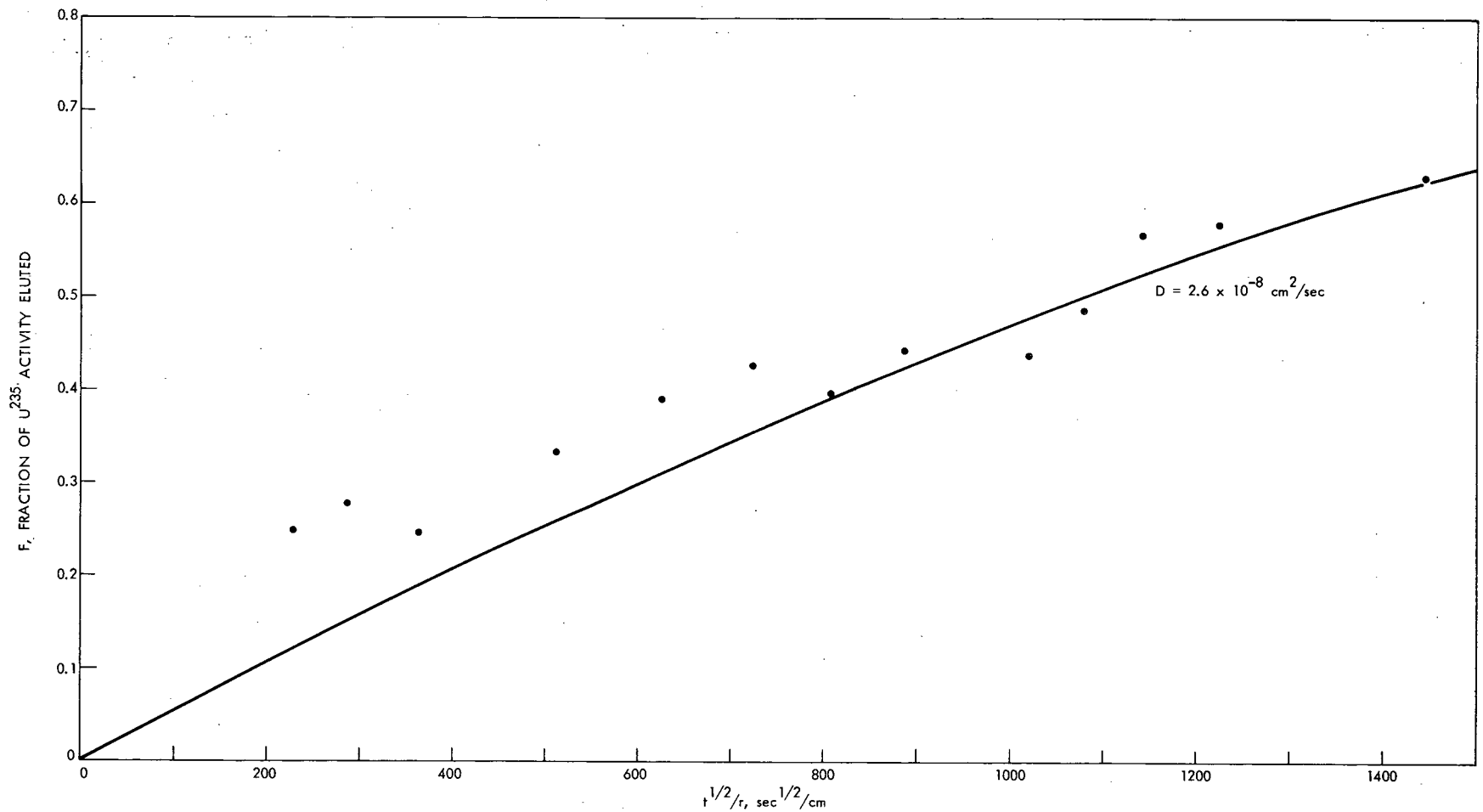


Fig. 5.2. Self-diffusion of uranyl sulfate in 960 μ Dowex 21K with a solution flow rate of 17 cm/sec.

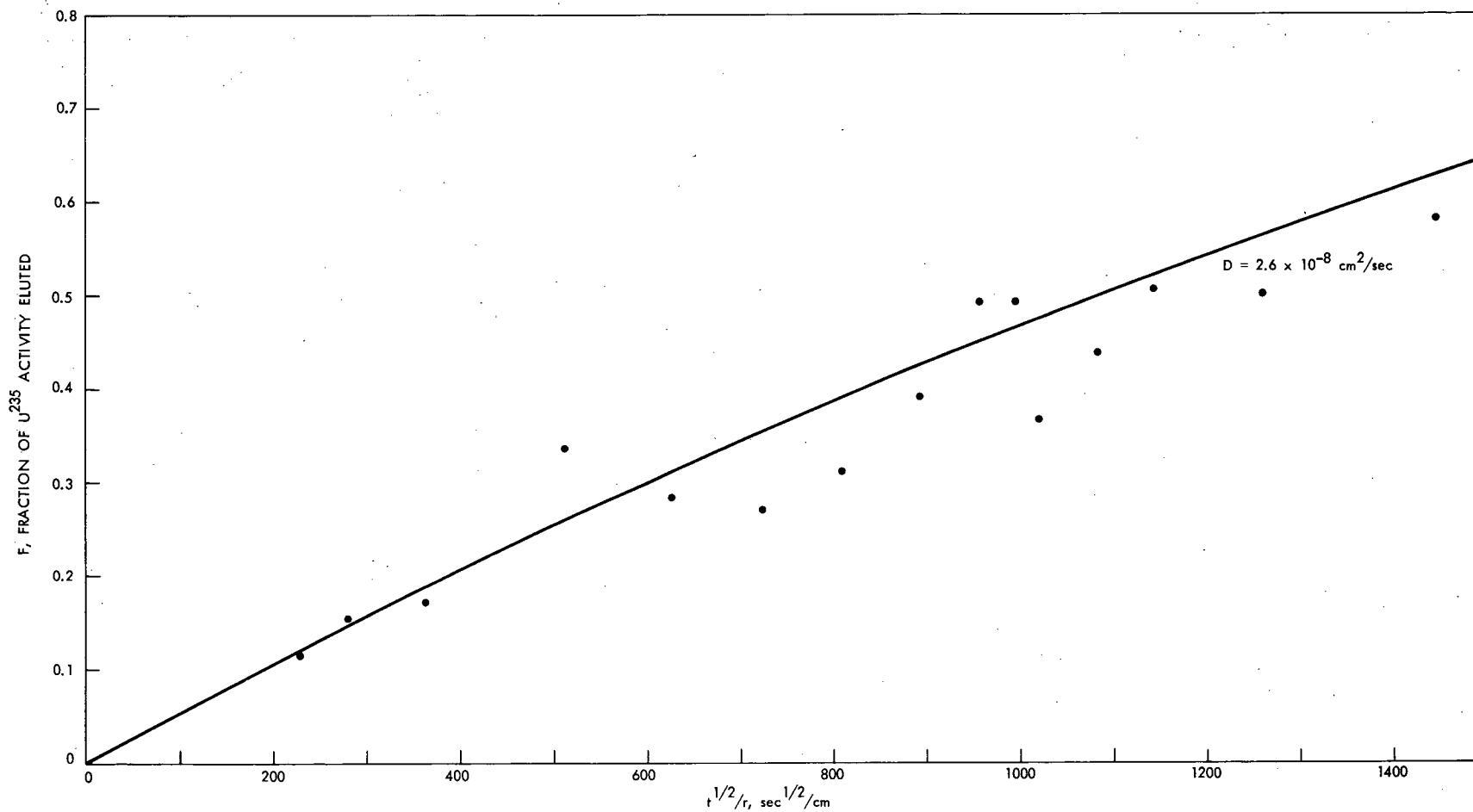


Fig. 5.3. Self-diffusion of uranyl sulfate in 960 μ Dowex 21K with solution flow rate of 19 cm/sec.

ORNL-LR-DWG. 51323
UNCLASSIFIED

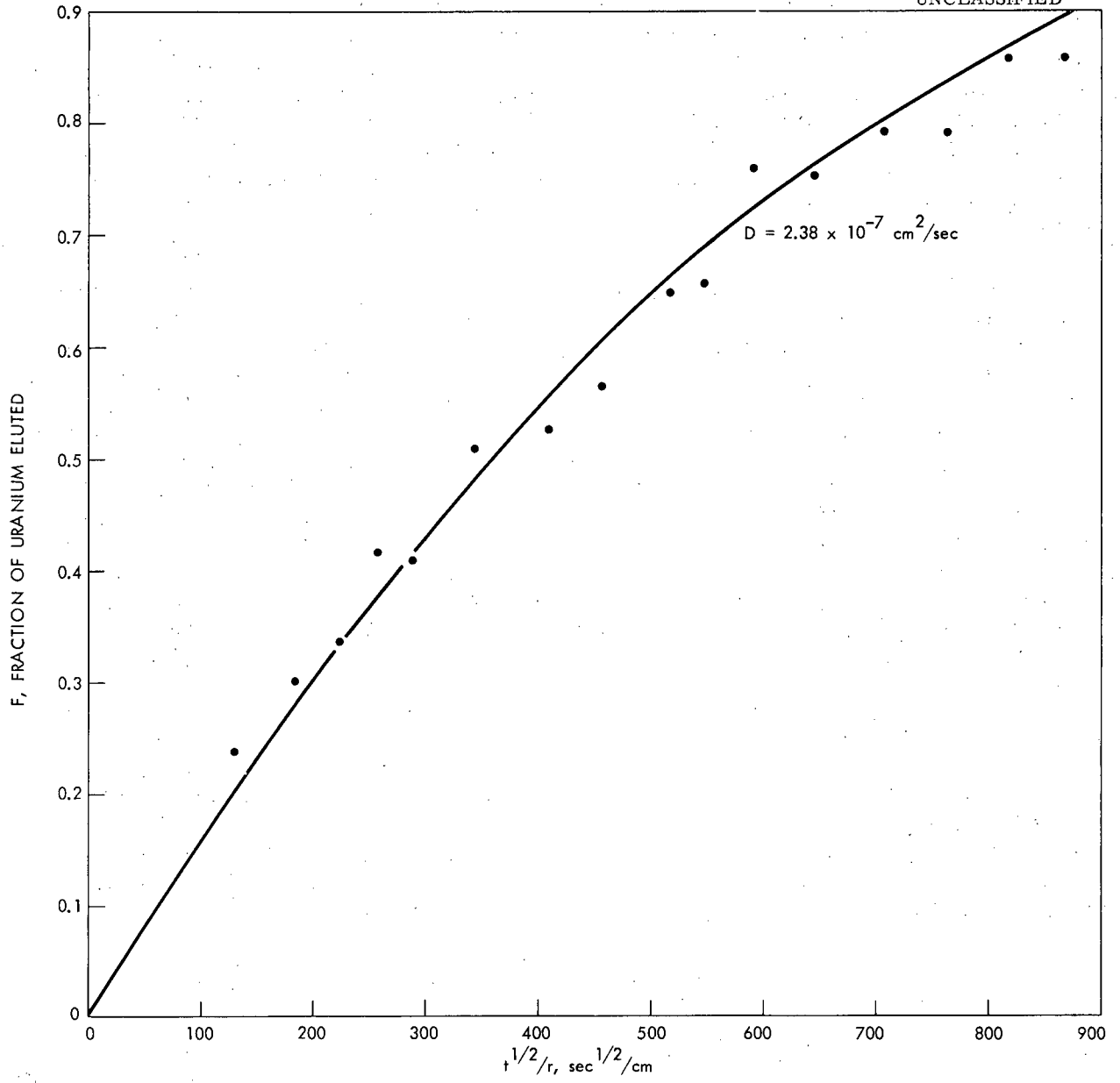


Fig. 5.4. Chloride elution of 1200 μ Dowex 21K.

6.0 POWER REACTOR FUEL PROCESSING

C. D. Watson

6.1 Darex-Thorex - F. G. Kitts

The purpose of the Darex process is to convert stainless steel-containing fuels into chloride-free nitrate solutions suitable for processing in existing stainless steel equipment. Chloride is necessary to effect dissolution but must be removed to avoid corrosion of subsequent processing equipment. Presently Darex-Thorex is being evaluated for the processing of stainless steel clad UO_2 - ThO_2 fuels such as Consolidated Edison. After decladding with 5 M HNO_3 - 2 M HCl the ceramic core material is dissolved in fluoride catalyzed nitric acid. In the current investigation the effect of the extent of dissolution (per cent dissolved) on the instantaneous dissolution rates of UO_2 - ThO_2 pellets was studied.

In addition to the instantaneous dissolution rates previously reported (June 1960 Unit Operations monthly progress report), two groups of about fifty UO_2 - ThO_2 pellets previously 1 to 40 and $> 70\%$ dissolved were immersed in Thorex dissolvent (12 M HNO_3 , 0.04 M NaF , 0.1 $Al(NO_3)_3$, 0.2 M Th , 0.01 M U) for appropriate times to produce weight losses of ~ 50 mg. Reaction rates (mg/g-min) were calculated and plotted vs % dissolution in Figure 6.1. Also plotted in Figure 6.1 are the data reported in tabular form last month covering ranges of % dissolution of 0-1 and 33-70%; therefore, Figure 6.1 presents over 300 data points covering from 0 to 87% dissolution. It was expected that the reaction rate would rise sharply as 100% dissolution was approached since the surface/mass ratio increases, but the intermediate maximum in the 12-16% range cannot be satisfactorily explained. This may have been caused by small particles of UO_2 - ThO_2 dropping from the pellet surface and being observed as a weight loss without actually dissolving.

With the relationship between dissolution rate and % dissolution fairly well defined at a particular dissolvent composition (it is assumed proportional at other compositions) some further work was done with the data relating initial dissolution rate and dissolvent composition. In the initial correlation of these properties the reaction rates were expressed as mg/cm^2 -min (May 1960 Unit Operations monthly progress report); the same data were replotted and refitted (only minor revisions) to yield reaction rates expressed as mg/g-min when calculated by the following expression (Figure 6.2):

$$R = 0.627 \left(\frac{HNO_3}{10} \right)^3 - 0.336 \left(\frac{HNO_3}{10} \right)^4 - 0.12 \left(\frac{HNO_3}{10} \right)^3 Th$$

where R = reaction rate, mg/g-min

HNO_3 = nitric acid molarity

Th = thorium molarity

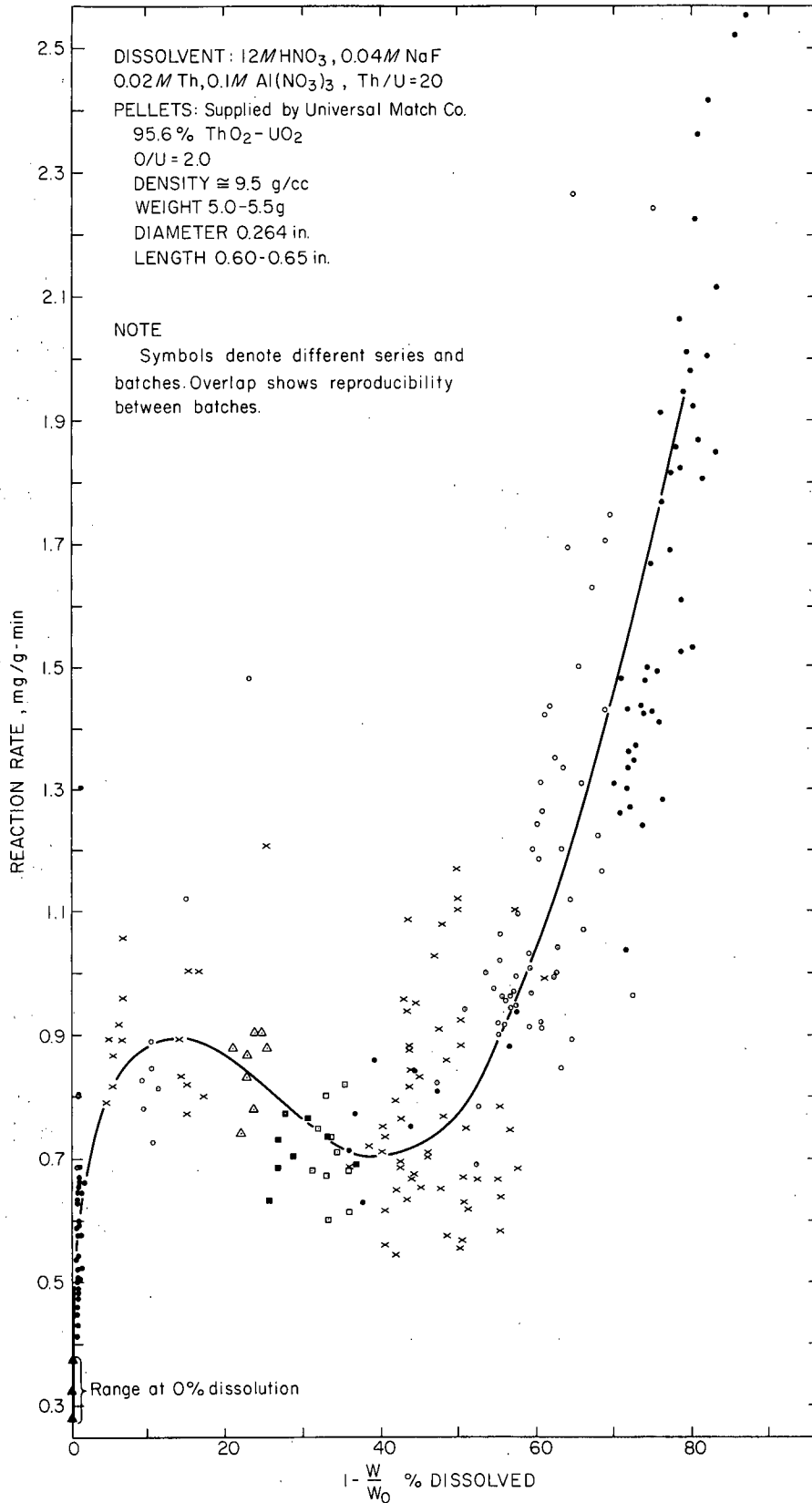


Fig. 6.1. Reaction rate of single UO₂-ThO₂ pellets as a function of fraction dissolved.

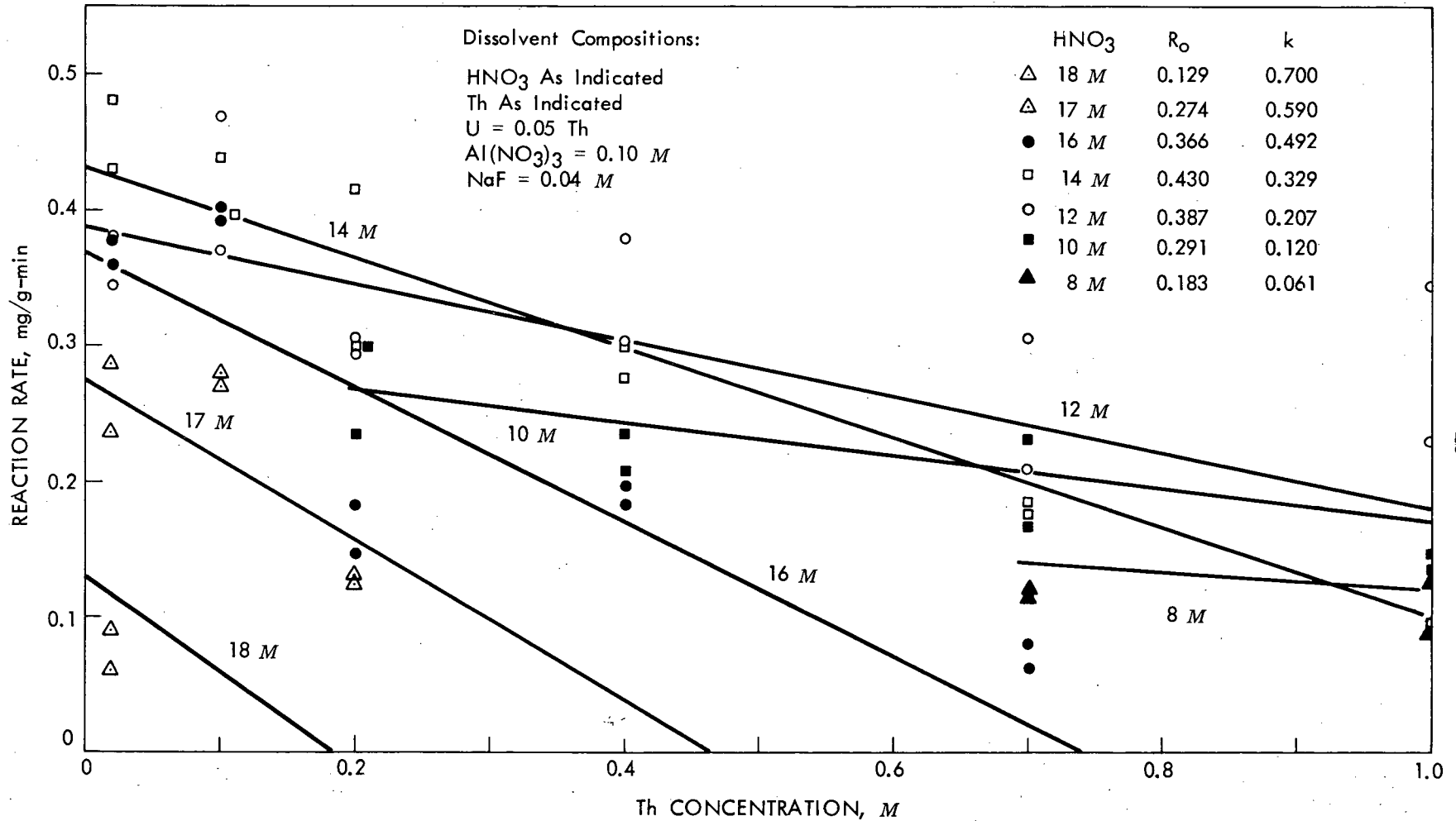


Fig. 6.2. Correlation of reaction rate (mg/g-min) with dissolvent composition.

$$R = 0.627 \left(\frac{\text{HNO}_3}{10} \right)^3 - 0.336 \left(\frac{\text{HNO}_3}{10} \right)^4 - 0.12 \left(\frac{\text{HNO}_3}{10} \right)^3 \text{ Th}$$

In order to check the agreement between the experimental rates (designated E) and those calculated using the correlation (C), some arbitrary quantities were calculated. The average deviation

$$\frac{\sum_{i=1}^{i=n} (C_i - E_i)}{n} = - 0.0036 \text{ mg/g-min}$$

shows that the plus and minus variations from the correlation values were very nearly equal. The average mean square deviation

$$\sqrt{\frac{\sum_{i=1}^{i=n} \left[\left(\frac{C - E_i}{C} \right)^2 - \left(\frac{C - \bar{E}}{C} \right)^2 \right]}{n}} = 0.22$$

shows that there is considerable scatter in the data, but any true rate (E), with > 95% certainty, should lie within $C \pm 1/2 C$ where C is the rate calculated from the correlation.

6.2 Evaluation of Packed Process Tanks - B. A. Hannaford

Large capacity tanks, planned for critically-safe storage of fissile material, may incorporate a nuclear poison of randomly packed raschig rings of borosilicate glass. Satisfactory methods for solution mixing, liquid level determination, and removal of particulate solids must be demonstrated for such a packed vessel. In addition, observations must be made on attrition of the glass, change in void fraction, and leaching of boron.

Following mixing experiments in which a sparge ring was shown to be the best mixing device of those tested in the packed tank (June 1960 Unit Operations monthly progress report), an electrical conductivity probe in the packing was wired to provide a continuous record of solution resistance with time.

A preliminary mixing experiment was performed in which successively larger volumes of water were added to a dilute NaNO_3 starting solution followed each time by sparging with air until equilibrium was reached. The results of the first experiment are summarized in Table 6.1.

Conclusions to be drawn from the data depend strongly on the definition of "equilibrium" or approach to equilibrium desired. Because of the greater sensitivity of the present measuring technique, as compared with sample withdrawal, the mixing times are longer than previously reported.

Table 6.1. Time Required to Mix NaNO₃ Solutions and Water in a 200-gal (nominal) Tank (L/D ≈ 2) Packed with Glass Raschig Rings.^{a,b}

Initial Solution	Volume, gal		Equilibrium Time, ^c min	Equilibrium NaNO ₃ Conc. ^d <u>M</u>	Equilibrium NaNO ₃ Conc. (calc.) ^e <u>M</u>
	Water Added	Final Volume			
44	14	58	17	0.0079	0.0076
			50	0.0074	
58	27	85	23	0.0059	0.00587
85	65	150	7	0.0042	0.0042

^aMixing device: a 28-in. dia ring, containing 12 equally-spaced 1/16-in. dia holes, supported approximately 1-in. from tank bottom and 2-in. from tank wall. Air rate: 0.5 scfm/ft² of tank cross-section.

^bBorosilicate glass rings 1.5-in. o.d. x 1.75-in. long. Void fraction: 77.4%.

^cTime after which no perceptible change in concentration occurs at the probe.

^dAs calculated from the measured equilibrium resistance value.

^eIncludes the (NaNO₃) equivalence of the process water (~0.0020 M) used for dilution.

6.3 Mechanical Processing - G. A. West, G. K. Ellis, J. B. Adams, A. M. Benis

SRE Dejacketing Studies. The dejacketing equipment of the Cell A High Level Segmenting Facility was operated by remote means to demonstrate the feasibility of mechanically dejacketing the NaK bonded stainless steel clad SRE fuel rods at a reasonable production level (~200 kg U/day). Several clad runs made with SRE prototype fuel rods were highly successful.

The hydraulic dejacketing unit operated satisfactorily in processing SRE prototype fuel rods (containing steel slugs and no NaK bond) through each sequence of operation of (1) aligning and cutting through the 10 mil thick stainless steel (304L) clad to remove end caps, (2) expanding the jacket 80 mils with 1300 psig hydraulic pressure to simulate the procedure for removing swollen slugs, (3) ejecting the slugs with < 100 psig hydraulic pressure, and (4) the winding the 92-5/16-in. long jacket into a 3-1/2-in. dia spiral roll for disposal as scrap. Subsequent transferring and steam cleaning of the slugs in preparation for recanning and storage was accomplished without incident.

Multipurpose Disassembly Saw. The hydraulic powered disassembly saw performed satisfactorily after alterations were completed on the hydraulic system and a higher viscosity (226 SUS at 100°F) fluid substituted for the UCON Hydrolube AC which had too low a viscosity (58.5 SUS at 100°F), and in

sufficient lubricating qualities for the Vickers hydraulic pumps and motors. The new fire resistant hydraulic fluid, Shell IRUS No. 902, allows optimum performance of the hydraulic system when not exposed to radiation. However, radiation tests by a Co^{60} γ source show that the water and emulsifying agents are separated from the oil after 10^7 r, total dose. The results of viscosity measurements made on the bulk phase of the Shell IRUS No. 902 fluid after irradiation were as follows:

<u>Radiation Dose</u> (roentgens)	<u>Viscosity</u> (SUS at 100°F)
None (Control)	226
1×10^7	143
5×10^7	117
1×10^8	127
5×10^8	230

A fire resistant hydraulic fluid that is radiation resistant and possesses lubrication and viscosity requirements for the Vickers hydraulic pump is desired. Since the UCON Hydrolube AC was fire retardant and radiation resistant a proposal will be made to the manufacturer to supply UCONs for test with increased viscosity and additives to increase the lubricating properties, if this is possible.

Test of Cell A Fire Fighting Equipment. The cell is equipped so that a total of 20 cylinders, containing 75 lbs each of CO_2 , can be discharged to the cell to combat fires other than those of burning metals. The release system operates satisfactorily as demonstrated by a test conducted with the assistance of the ORNL Fire Department. Only 10 of the 20 CO_2 cylinders available were used in the test. The following effects were determined from the release of the CO_2 : (1) the internal cell pressure increases from a slightly negative pressure to a positive 5 in H_2O when the inlet damper is closed and the outlet damper set for minimum exhaust, (2) the pressure was a -0.6 in. H_2O with the exhaust damper full open, (3) the lowest oxygen content recorded was ~10%, (4) the internal cell temperature was reduced from 80°F to 24°F during the first minute of the maximum CO_2 release.

Leaching. 7.5-kg UO_2 was leached in 16.35 liter of 13 M HNO_3 in the intermediate size, natural convection leacher from 0.5-in.-dia 1-in. long stainless steel clad pieces sheared from a UO_2 filled assembly (Mark I). Excessive foaming occurred when the sheared fines from this quantity of UO_2 were suddenly contacted with boiling 13 M HNO_3 . Sudden immersion of sheared UO_2 fines in boiling concentrated HNO_3 is indicated as not being feasible. A departure from flow sheet conditions was necessary after 3-min of this fast reaction. Bulk UO_2 in the leach basket was pulled from the acid and heat supplied to the leacher was removed. Sixteen minutes later the UO_2 dissolution was continued with moderate foaming (30-40% reactants volume) to obtain further qualitative information at a lower initial acid temperature of 92°C. Foaming will probably not be a problem if the reaction of UO_2 fines is started immediately at room temperature. This requires the fines to be immediately wetted at room temperature by the acid. At this condition no foaming was observed in an earlier experiment reacting 1.2-kg sheared UO_2 (0.5-in. lengths) in 13 M HNO_3 (June 1959 Unit Operations monthly progress report).

At the end of this run, 12 g (0.16% of 7.5-kg charge) black, flocculent, flaky, low density (tap density 0.44) residue, probably carbonaceous, repeatedly plugged a 0.5-in.-dia liquid waste outlet draining the product. This may indicate a problem jetting HNO₃ insolubles, originating in the UO₂ fuels, from the leacher at the end of a run.

Shear-Leach Concept. Some of the most difficult criteria in the chop-leach remote complex are those primarily associated with solids material transfer:

1. Chopped pieces must be transferred from the shear to the leacher without spread of contamination, preferably without opening the leacher or shear to the cell atmosphere.
2. Access must be provided of acid to the fuel in the leacher.
3. Leached cylinders must be transferred from the leacher to disposal.

These criteria may possibly be met using a modified version of the "H" leg leacher (February 1959 Unit Operations monthly progress report) shown in Figure 6.3. Sheared ceramic core pieces would be dropped directly into the leacher simplifying this transfer operation. UO₂ fines would be immediately accessible to acid and it would never be necessary to open the shear or leacher to cell atmosphere. The UO₂ transfer bucket, aluminum foil liner and bucket transfer mechanism would be eliminated. This concept becomes practical if (1) solids bridging or jamming in the 10-in.-dia leacher leg is no problem, and (2) it is possible to maintain and operate a valve in the bottom of the leacher through which to remove leached and washed rings for disposal. A vertical 10-in.-dia 8 ft long cylinder has been set up to access the bridging-jamming problem simulating the existing "H" leg leacher side arm. The valve in the bottom of the leacher may probably be maintained and operated because during the leaching operation it is separated by a gas lock from the liquid acid and it is cooled by an entering gas stream. Oxygen or air purge gas needed in the leaching off-gas stream to oxidize NO is inserted continuously during leaching (position A) in the bottom of the 10-in.-dia leaching cylinder. Acid vapor corrosion of valve surfaces should be negligible because the pressure in the gas space will suppress the liquid vapor pressure below the boiling point at the gas-liquid interface. Leached cylinders would be transferred from the leacher to disposal container in position B after the uranyl nitrate solution had been jettted out, leached rings washed, and wash liquor jettted out. The position change necessary to make the solids transfer would be made by swiveling the bottom valve 180° about a Grayloc clamp type joint connection. Metal pieces adhering around the valve seat would be washed out into the disposal container, the valve closed, disposal container removed at a second Grayloc connection, and a Grayloc vessel closure installed on the container before removing it to disposal. The leaching-disposing cycle would then be repeated. At no time would the shear or leacher be open to the cell atmosphere.

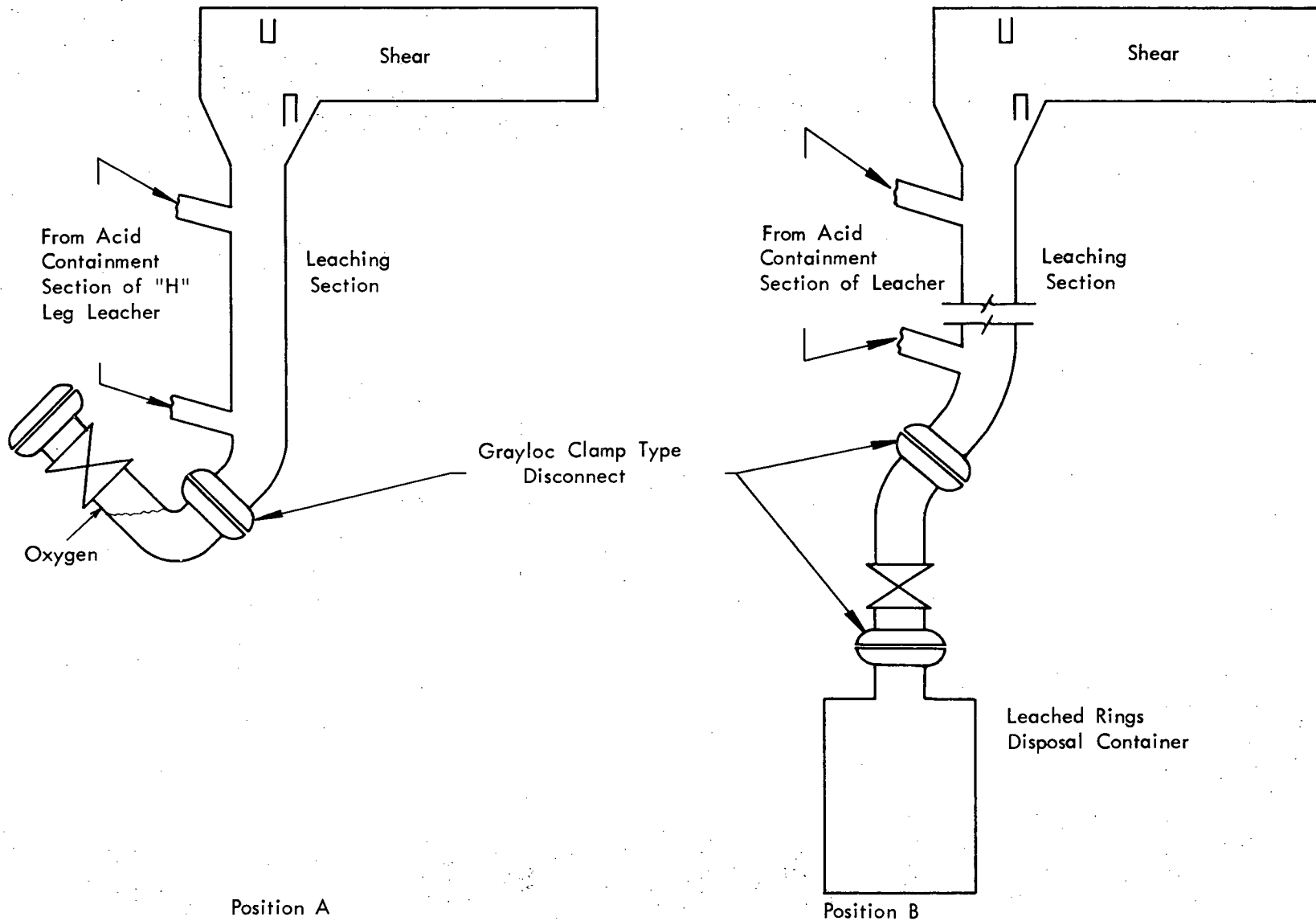


Fig. 6.3. Concept of chop-leach arrangement.

Shearing. A 3-ft section of stainless steel clad, porcelain loaded, Yankee prototype subassembly (36 0.337-in.-dia tubes) with Kanigan-brazed, diffusion-bonded joints was sheared using an "M" shaped punch and 90° anvil. At one of two ferrule locations sheared, five 2-tube pieces and one 5-tube piece remained integral after cuts into 1-in. lengths (Figure 6.4). The largest piece of a prototype Mark I (36 0.5-in.-dia tubes), shearing under the same conditions was one 2-tube piece.

Wear by forging and galling of blade surfaces after only 18 cuts was appreciable (Figure 6.5) but is probably to be expected at the generally low Rockwell C53 hardness. Rockwell C59 was the specification hardness. There was greatest wear in the vicinity of the two lowest observed hardness values of Rockwell C41 and 48.

There will probably be no appreciable difference in fines size distribution shearing different diameters of tubes in ceramic filled fuel bundles. This is indicated in Figure 6.6 comparing the porcelain and metal size distribution of fines from shearing subassemblies representative of the Nuclear Ship Savannah and Yankee fuels.

A Mark I ceramic core prototype containing ferrules on 4-in. spacing with ductile heliarc ferrule-to-tube welds was sheared using an "M" shaped punch and vee anvil. This experiment showed the maximum effect a ductile weld may have producing agglomerate sheared pieces. Large integral pieces incompatible with operation of the continuous leachers in this program were produced from all of 4 ferrule cuts (Figure 6.7). The largest piece is shown in more detail in Figure 6.8. This indicates future development of brazing techniques may significantly affect the ability of the shear to produce discrete single pieces.

Alternate Disassembly and Ceramic Exposition Methods. A 4-in. long section of a Mark I element containing one ferrule section of 25 tubes was disassembled into slabs under oil (Figure 6.9) in 4 hrs with an electrical discharge type machine (maximum 40 volts between electrode and work) using as an electrode a 1/32-in. thick copper sheet. The excessive time required is the disadvantage of this technique but this might be minimized using a higher powered machine.

In slabs of one or two tubular element layers the ceramic core may easily and quickly be exposed without apparent appreciable alloying and envelopment of the ceramic (Figure 6.10) by "hot-rodding". A direct current welding machine is used with reverse polarity current of 350-400 amps and a mild steel coated rod. Thirty-six holes of the kind shown here may be made before a rod is consumed. There is a possibility of using a non-consumable electrode.

The mechanical feasibility of using the underwater constricted arc torch will be tested immediately trying, without precise torch positioning, to reduce a recently fabricated 4 x 4 square array bundle of stainless clad porcelain in 0.5-in.-dia tubes to rubble. A similar experiment on a 4.5-kg size UO₂ filled bundle has been planned to obtain a product to test the HNO₃ accessibility of the UO₂ alloyed and enveloped in stainless steel residue from such cutting operations. The delay has been caused by limited manpower allocation.

UNCLASSIFIED
PHOTO 50648



Operating Conditions:
Shear - 150 ton vertical driven
Blade - Material, Carpenter 610
- Velocity, 2 in./sec
- Type, plane of contact
- Hardness, Rockwell C-53

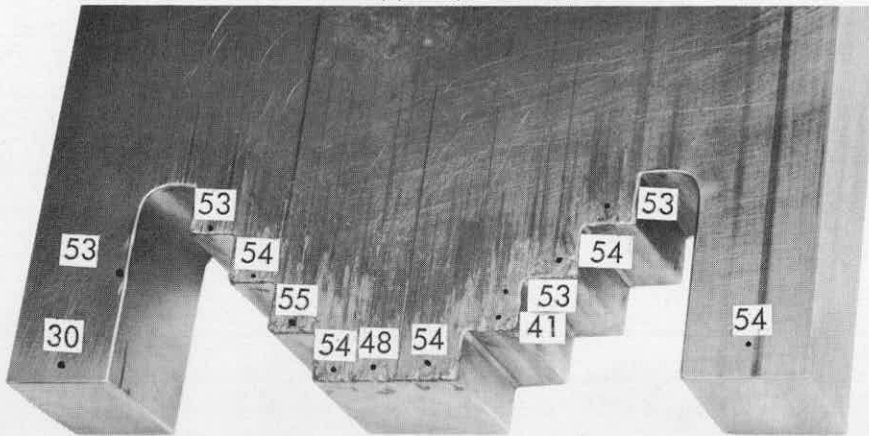
Fig. 6.4. Integral pieces remaining after one shearing cut at a ferrule section of a Yankee prototype porcelain filled subassembly (36 - 0.337 in. dia tubes).

Operating Conditions:

- Shear - 150 ton vertical driven
- Blade - Material, Carpenter 610
 - Velocity, 2 in./sec
 - Type, plane of contact

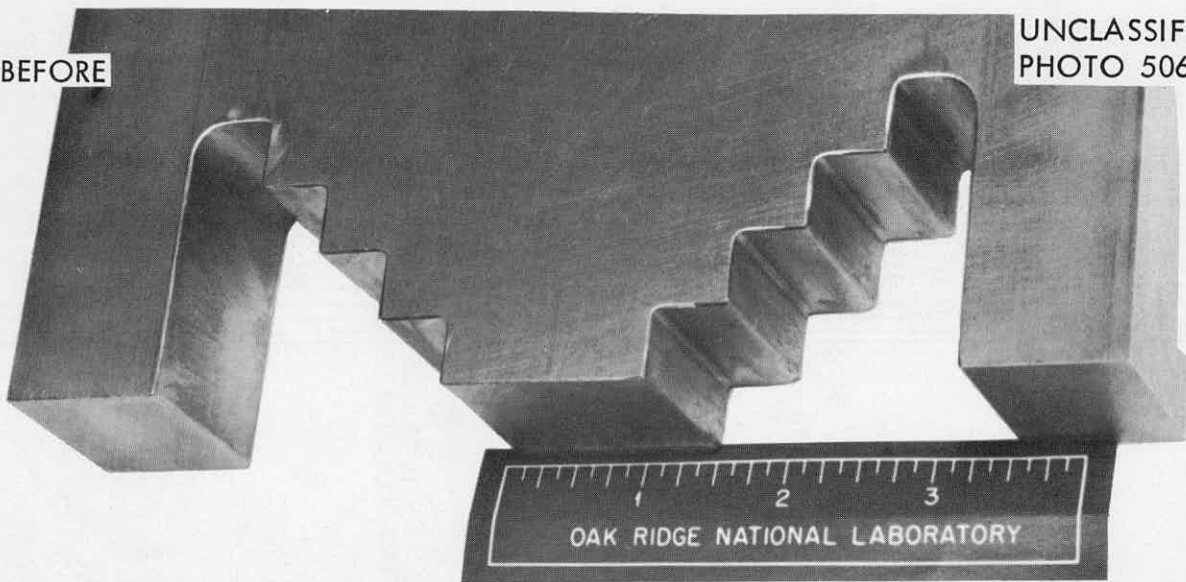
UNCLASSIFIED
PHOTO 50646

AFTER



BEFORE

UNCLASSIFIED
PHOTO 50647



• Blade Hardness - see numbers on blade edge
(Rockwell C Scale)

Fig. 6.5. "M" shaped punch before and after 18 shears of a Yankee porcelain filled subassembly (36 - 0.337 in. dia tubes).

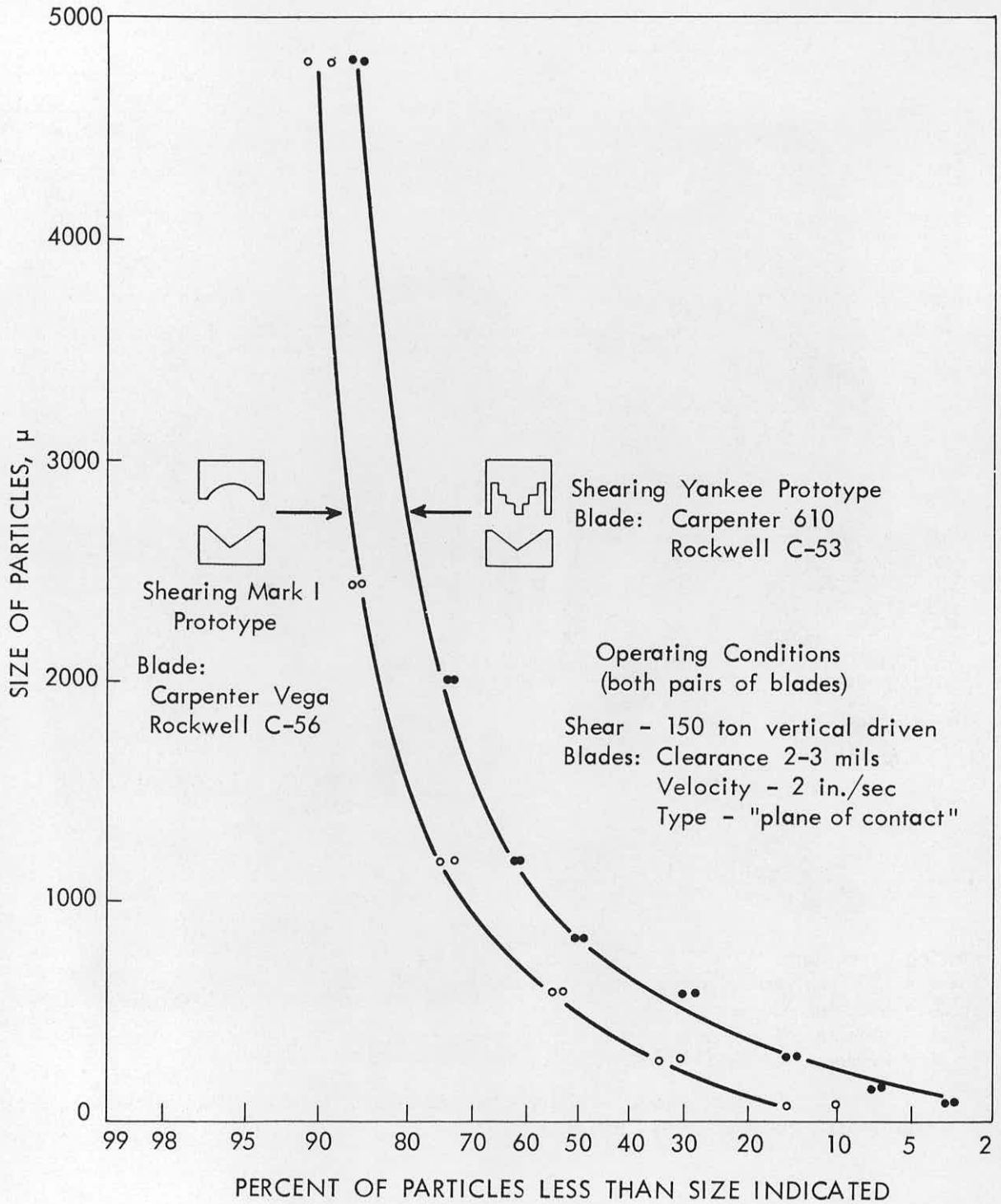
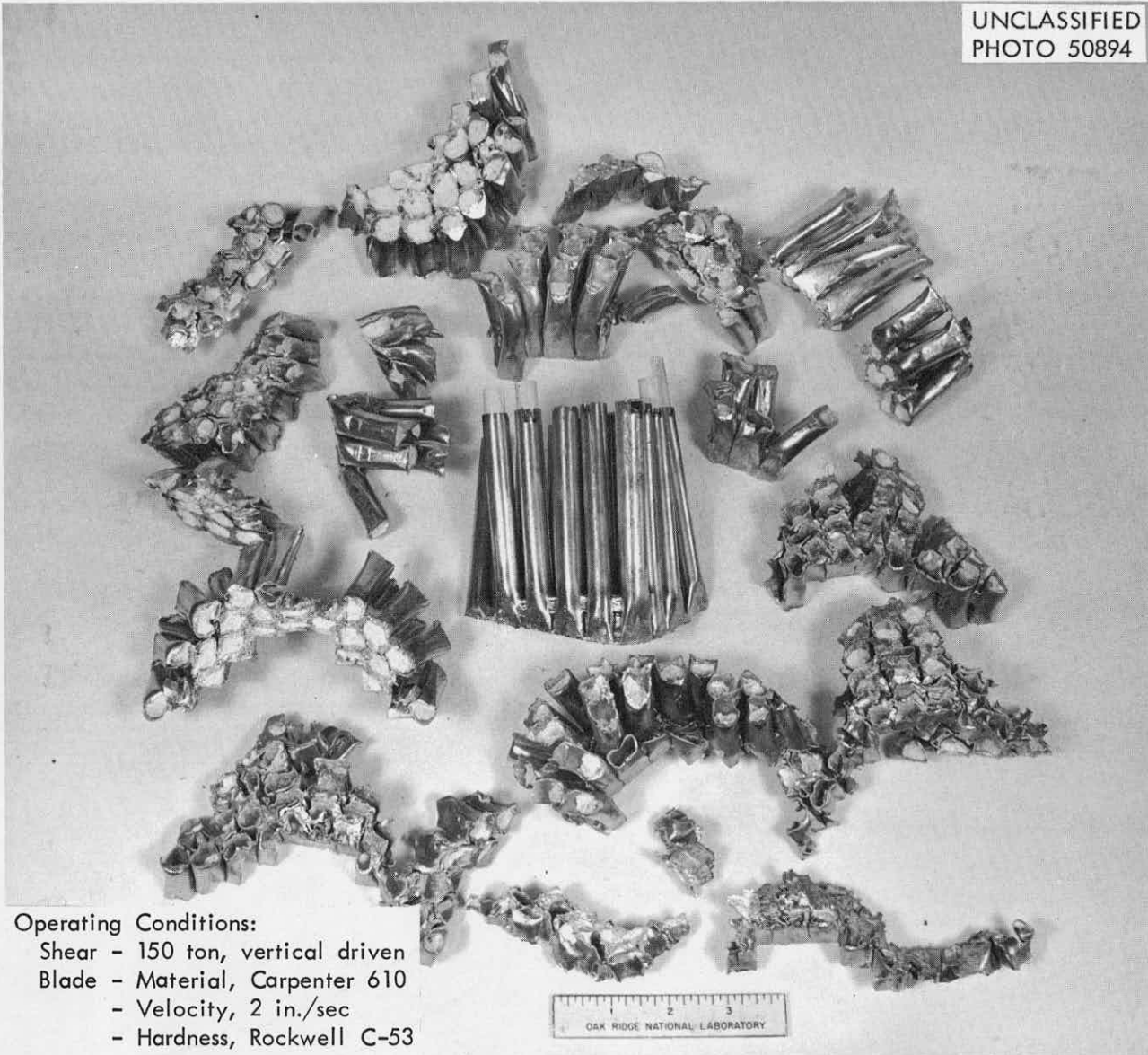


Fig. 6.6. Comparison of sheared product (porcelain and metal) size distribution from shearing Nuclear Ship Savannah (represented by Mark I) and Yankee stainless-clad porcelain-filled subassemblies.

UNCLASSIFIED
PHOTO 50894



Operating Conditions:
Shear - 150 ton, vertical driven
Blade - Material, Carpenter 610
- Velocity, 2 in./sec
- Hardness, Rockwell C-53

Fig. 6.7. Integral pieces remaining after shearing at four ferrule locations of a ductile brazed Mark I porcelain filled assembly.

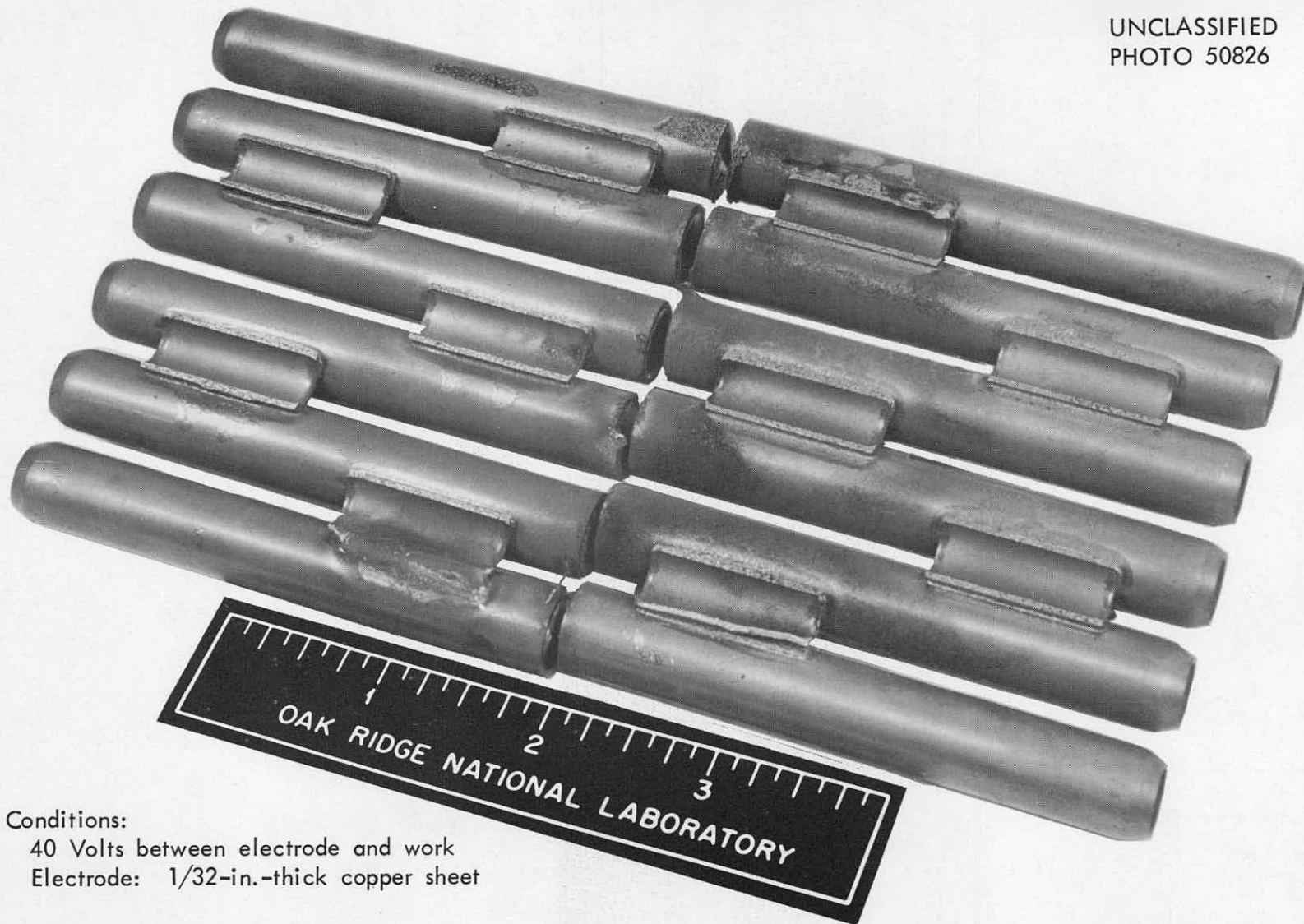
UNCLASSIFIED
PHOTO 50823



Operating Conditions:
Shear - 150 ton vertical driven
Blade - Material, Carpenter 610
- Velocity, 2 in./sec
- Type, plane of contact
- Hardness, Rockwell C-53

Fig. 6.8. The largest piece remaining from shearing at four ferrule locations of a ductile brazed Mark I porcelain filled assembly.

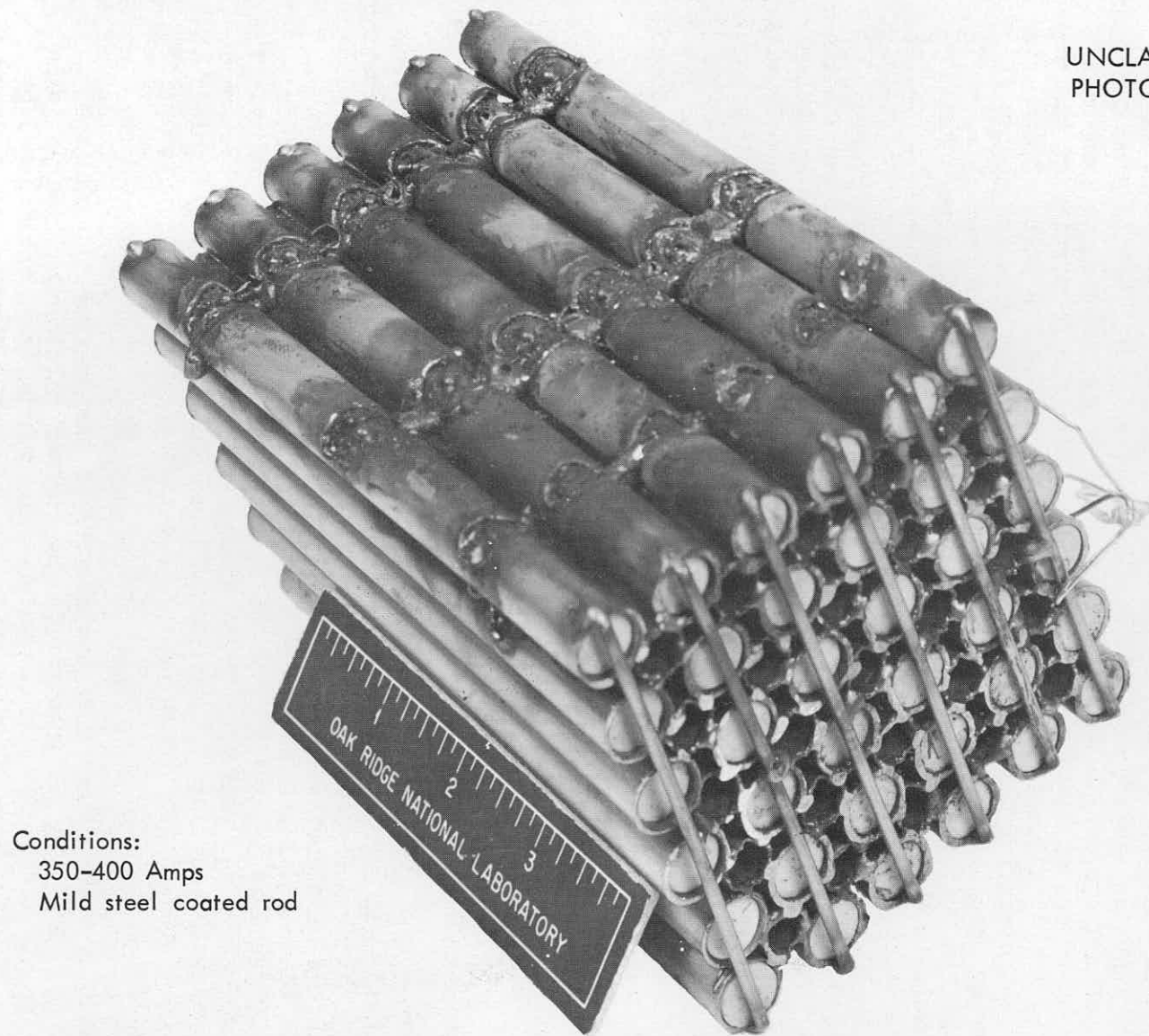
UNCLASSIFIED
PHOTO 50826



Conditions:
40 Volts between electrode and work
Electrode: 1/32-in.-thick copper sheet

Fig. 6.9. Characteristic slabs from disassembly of 6 x 6, 0.5-in.-dia tube bundle using an electrical discharge type machine.

UNCLASSIFIED
PHOTO 50825



Conditions:
350-400 Amps
Mild steel coated rod

Fig. 6.10. Exposition of ceramic core in a Mark I 6 x 6 layer of 0.5-in.-dia tubes using reverse polarity current from a direct current welding machine.

Cost Study. A preliminary cost study has been initiated to evaluate the relative economics of mechanical (chop and leach) versus aqueous (declad-core dissolution) processing of stainless steel clad, ceramic fuels. The cost study will be used to evaluate the ultimate usefulness of the chop-leach concept in fuel processing and as an aid in directing the emphasis of subsequent development programs.

Sufficient development work has been performed at ORNL to produce a shear design that is believed to have the capability of performing the desired function satisfactorily. The cost estimate will be based on the design of a large single purpose plant with a capacity equal to that of a single shear operating on a single fuel type with the properties of the NMSR (nuclear ship), a large cross section, tubular bundle. A plant of such size (~3 tons U/operating day) might be feasible after 1975 when the number of fuel types should be reduced and large amounts of fuel are available, although the fuel type may not be SS clad-ceramic as chosen here. This will evaluate the shear concept under favorable conditions since the capital and operating costs of a shear for bundles of tubes (in the range of 2-in. x 2-in. to 10-in. x 10-in. rectangular dimensions) are rather inflexible functions of its production rate which varies mainly with the cross section of the bundle chopped. The shearing rate is in the range of 4-6 strokes per minute; loading and cleaning times are about equal regardless of bundle size.

Alternate declad-core dissolution processes (Sulfex, Darex) will be compared at equal capacity. The particulate nature of the chopped feed (~1/2-in.-dia x 1-in. long pieces) allows the advantage of using continuous dissolution equipment as opposed to multiple batch required with declad-core dissolution processes. Solvent extraction and off-gas systems should be essentially identical for both types of plants. Waste disposal facilities, however, will be much more extensive for decladding solutions than for solid stainless steel waste.

6.4 Radiation Damage Studies - G. A. West

Ninety-one protective coatings were exposed to ionizing radiation from both inside and outside of the thermal shield during 9,030 hours of operation of the HRE. These were inspected for radiation damage and pickup and retention of radioactive particles. The protective coatings inside and outside the thermal shield were exposed to a total dosage of 4.9×10^8 r, 1.1×10^8 r and temperatures of 40 to 60°C and 30 to 50°C, respectively. The coatings were under water for 5,952 hours (~59 weeks) during the test period. Prolonged water exposure was not anticipated and it is highly probable that failure of some of the "house paint" type coatings resulted from immersion alone.

Initial observations indicate that 25 of the coatings outside the shield and 10 of the coatings inside the thermal shield exhibited satisfactory resistance to both radiation and water. The panels were contaminated by activity escaping from disconnects during underwater maintenance procedures. The maximum activity detected on the panels before the decontamination washes was approximately 1,000 mrep/hr. The activity remaining after scrubbing these test panels, using both a detergent and citric acid, ranged from 0.1 to 40 mrep/hr with an average of 5 mrep/hr. A complete evaluation of the various coatings will be made after additional physical tests are completed.

7.0 SOLVENT EXTRACTION STUDIES

A. D. Ryon

The HETS values for thorium extraction reported this month were obtained as part of the overall solvent extraction studies designed to assist in the adaptation of TBP process to the reprocessing of various power reactor fuels. A description of the compound extraction-scrub columns used in this study may be found in the October 1959 Unit Operations monthly progress report (CF 59-10-77), while a description of the acid Thorex flowsheet may be found in the April 1960 Unit Operations monthly progress report, (CF 60-4-37).

7.1 HETS Values for Thorium Extraction - Acid Thorex Flowsheet - R. S. Lowrie, F. L. Daley

HETS values for thorium extraction were obtained for both aqueous (top interface) and organic (bottom interface) continuous operation of a sieve plate column (0.125-in.-dia holes, 23% free area) and for organic-continuous operation of two nozzle plate columns (0.125-in.-dia nozzles, 10% free area and 0.188-in.-dia nozzles, 23% free area). Operating conditions were those for the acid Thorex flowsheet: a Purex-type extraction system intended for use with Consolidated Edison-type fuels, employing 30% TBP in Amsco 125-82 as the solvent to co-extract uranium and thorium, a feed ≈ 0.1 M acid deficient, a dual scrub and the addition of a salting acid (14 M HNO_3) near the mid-point of the extraction section of the column. The operating procedure described below was the same regardless of the continuous phase or column cartridge (sieve or nozzle plates) being tested.

The feed, water (AS₁) and 5 M nitric acid (AS₂) scrubs, 14 M nitric salting acid and solvent (AX) flows were started, the pulse frequency set and the column allowed to reach steady state, indicated by a constant specific gravity in the loaded organic stream (AP). Timing of the run was then started and hourly samples were taken as follows: AP and AW (raffinate) streams for the first three hours and AP, AW, and column profile samples (see Figure 7.1 for location of profile sample points) for the next three hours. Hourly readings were also taken of all tank levels allowing an integrated flow rate to be calculated for each stream. The experimental conditions for the HETS runs are shown in Table 7.1 and the average analytical results for the flowing stream and profile samples are shown in Tables 7.2, 7.3, 7.4 and 7.5.

7.2 Calculation of HETS Values for Thorium Extraction

From equilibrium and material balance data, the number of theoretical stages required to obtain a desired raffinate value starting from any particular sample point of interest may be calculated by means of a McCabe-Thiele diagram. The HETS value can, in turn, be calculated by dividing the number of theoretical stages into the length of column between the two sample points. Equilibrium data for the thorium nitrate-30% TBP solvent-nitric acid system used in the McCabe-Thiele diagrams were from Sidall,¹

¹T. H. Sidall III, "The Extraction of Thorium Nitrate from Nitric Acid by TBP-'Ultrasene'", DP-181, October 1956, E. I. duPont de Nemours Co.

UNCLASSIFIED
ORNL-LR-DWG 51328

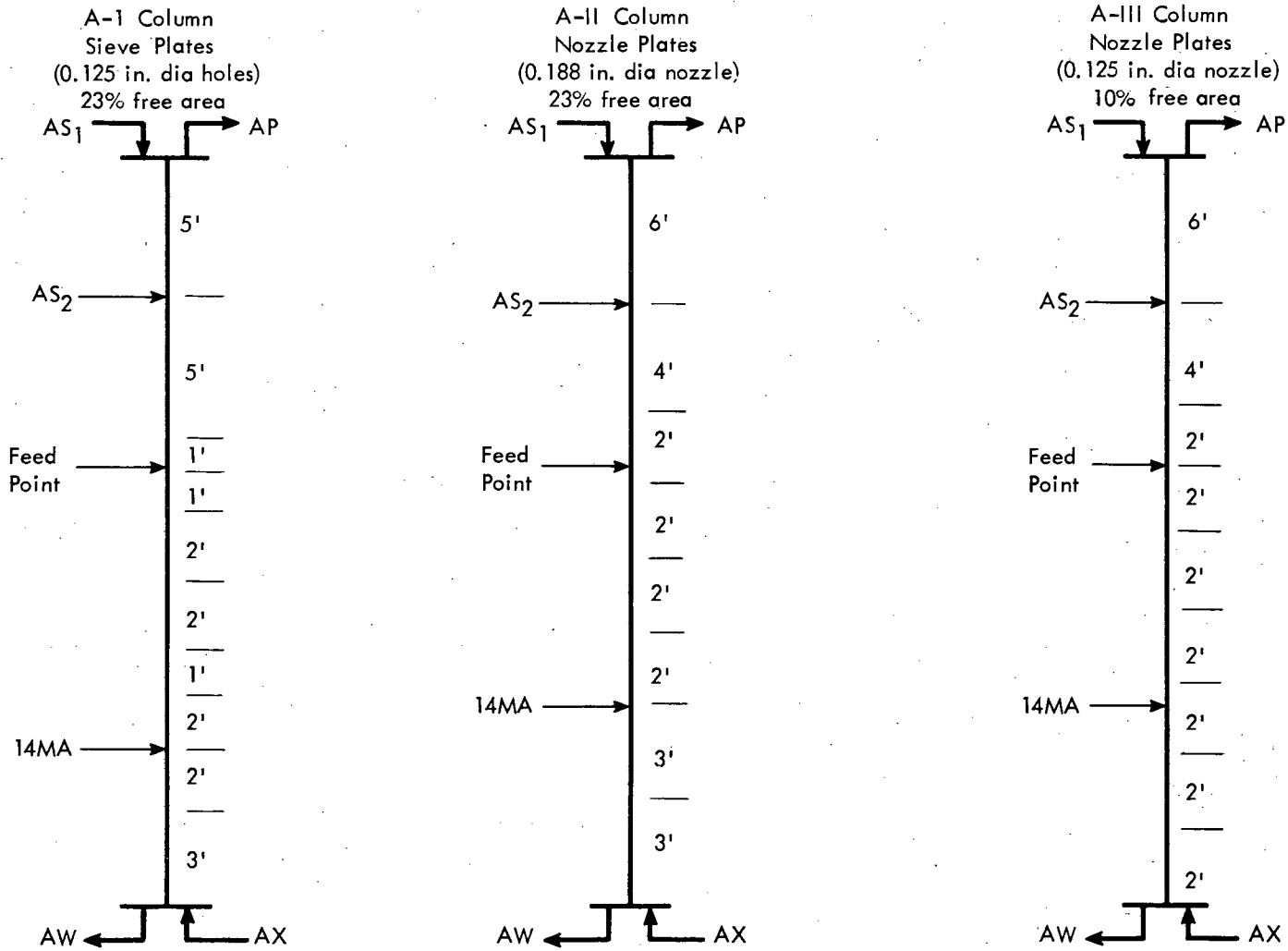


Fig. 7.1. Location of profile sample points in the extraction columns, Bldg. 3503, acid Thorex flowsheet.

Table 7.1. Experimental Conditions - HETS Runs

Pulse amplitude: 1.0 in.
 Pulse frequency: 50 cpm
 Temperature range: 23° - 28°C

Run No.	Phase	Flow Rates, gal/sq ft/hr							Total
		AS ₁	AS ₂	Feed	14 MA	AX	AP	AW	
Sieve plate column									
AT-2	Aqueous	49.8	13.9	54.1	31.9	414	439	125	564
AT-3	Aqueous	47.1	12.8	57.5	13.7	410	428	112	541
AT-23	Organic	48.5	11.9	60.3	27.5	413	422	140	562
Large nozzle plate column									
AT-17	Organic	82.5	18.8	105.0	56.8	649	684	229	913
Small nozzle plate column									
AT-14	Organic	84.3	19.6	93.6	57.3	717	737	240	972
ATP-2	Organic	47.0	12.8	59.5	33.3	421	444	130	573
ATP-8	Organic	49.2	18.7	80.7	12.7	422	428	155	583

Table 7.2. Average Analyses of Flowing Stream Samples HETS Runs

Run No.	AS ₁		Feed			14 MA	AX			AP			AW		
	H+ <u>M</u>	H+ <u>M</u>	U g/l	Th g/l	H+ <u>M</u>	H+ <u>M</u>	U g/l	Th g/l	H+ <u>M</u>	U g/l	Th g/l	H+ <u>M</u>	U g/l	Th g/l	H+ <u>M</u>
AT-2	0	4.8	19.6	235	0.13 AD	13.8	0.024	0.005	0.002	2.59	32.2	0.16	0.001	0.082	3.21
AT-3	0	4.8	19.6	235	0.13 AD	13.8	0.024	0.005	0.002	2.05	32.0	0.15	0.002	0.31	2.00
AT-23	0	4.8	20.1	246	0.11 AD	13.8	0.001	0.005	0.003	2.28	33.0	0.14	<0.001	1.42	2.70
AT-17	0	5.5	20.7	246	0.06 AD	13.4	0.002	<0.005	0.002	3.02	36.7	0.10	0.0004	1.80	3.14
AT-14	0	4.8	19.3	234	0.06 AD	13.8	0.001	0.008	0.002	2.79	31.3	0.14	0.001	0.129	2.80
ATP-2	0	5.0	19.3	234	0.06 AD	13.8	<0.001	0.005	0.002	2.38	33.1	0.15	<0.001	0.036	3.04
ATP-8	0	5.9	19.9	232	0.16 AD	13.8	0.074	0.003	0.027	4.71	44.0	0.08	0.006	0.27	1.9

Table 7.3. Analysis of Profile Samples, HETS Runs in Sieve Plate Column

Location of Sample Point ft from feed point	AT-2		AT-3		AT-23			
	Aqueous		Aqueous		Aqueous ¹		Organic	
	Th g/l	H+ M	Th g/l	H+ M	Th g/l	H+ M	Th g/l	H+ M
+1	62.2	1.2	63.7	1.3	-	-	-	-
Feed point	142.0	-	143.0	-	161.0	-	42.9	-
-1	56.3	1.1	60.0	1.1	127.0	1.1	36.2	0.30
-3	13.8	1.6	14.9	1.8	42.2	1.9	11.7	0.50
-5	4.36	2.5	3.61	2.3	15.5	2.4	4.0	0.65
-6	2.57	2.9	2.1	2.8	10.1	2.5	2.47	0.70
-8	0.43	5.6	0.80	4.1	4.47	5.1	1.04	0.90
-10	-	-	0.19	4.4	2.97	4.6	0.53	0.65
-13	0.13	3.1	0.22	2.1	1.74	3.7	0.13	0.34

¹Calculated by material balance from organic phase values.

Table 7.4. Analysis of Profile Samples, HETS Runs in Large Nozzle Plate Column

Location of Sample Point ft from feed point	AT-17			
	Aqueous ¹		Organic	
	Th g/l	H+ g/l	Th g/l	H+ g/l
+2	63.2	1.9	46.0	0.24
Feed point	155.0	0.8	46.8	0.23
-2	60.8	1.4	18.1	0.50
-4	15.2	2.1	4.57	0.72
-6	11.2	5.2	3.37	0.74
-9	3.64	5.1	0.66	0.68
-12	2.15	3.8	0.13	0.23

¹Calculated by material balance from organic phase values.

Table 7.5. Analyses of Profile Samples, HETS Runs in Small Nozzle Plate Column

Location of Sample Point ft from feed point	AT-14				ATP-2				ATP-8			
	Aq ¹		Org		Aq ¹		Org		Aq ¹		Org	
	Th g/l	H+ M	Th g/l	H+ M	Th g/l	H+ M	Th g/l	H+ M	Th g/l	H+ M	Th g/l	H+ M
+2	59.6	1.6	39.7	0.24	68.0	1.9	41.2	0.26	116.0	1.7	62.4	0.09
Feed Point	149.0	0.7	39.8	0.22	158.0	0.9	42.5	0.22	181.0	0.8	62.7	0.07
-2	17.4	1.5	4.60	0.65	20.5	1.2	5.50	0.52	152.0	1.3	52.5	0.23
-4	8.2	2.0	2.19	0.74	5.90	1.5	1.59	0.65	48.7	2.0	16.7	0.46
-6	2.67	5.8	0.84	0.93	2.65	2.7	0.81	0.91	9.09	3.9	3.27	0.76
-8	1.42	5.8	0.47	0.99	0.78	6.3	0.23	1.0	3.73	4.1	1.28	0.85
-10	0.82	5.6	0.23	0.92	0.20	6.1	0.057	0.95	0.60	3.8	0.122	0.73
-12	0.48	4.0	0.12	0.38	0.07	4.1	0.018	0.34	0.48	2.5	0.075	0.26

¹Calculated by material balance from organic phase values.

Codding,² and Rainey.³ The addition of a salting acid at approximately the mid-point of the extraction section of the columns (Figure 7.1) complicates the actual construction of a McCabe-Thiele diagram in two ways. First, unlike the basic Purex flowsheet (discussed in the January 1960 Unit Operations monthly progress report, CF 60-1-49) the aqueous acid concentration changed markedly over the entire extraction section (Figure 7.2), necessitating the use of "floating" equilibrium lines, dependent on both the acid and thorium concentration expected in any particular stage being stepped off. Second, the ratio of the aqueous flow to the organic flow (A/O), by definition the slope term in the equation for the operating line $[y_n = A/O (X_{n+1} - X_w) + y_0]$, changes at the point where the salting acid is added. This necessitates the use of two operating lines of slightly different slope which intersect at a point corresponding to the conditions present in the column at the salting acid feed point. A typical McCabe-Thiele diagram illustrating the use of the "floating" equilibrium curves and intersecting operating lines is shown in Figure 7.3.

No HETS values were determined for uranium extraction since almost all of the uranium was extracted before the first sample point (Figure 7.2), preventing the calculation of accurate HETS values.

HETS calculations were also affected by the profile sampling technique since the acid-thorium values obtained enter directly into the calculations. Although both aqueous and organic phase samples were taken at most profile points, the differential samplers operated in such a manner that the continuous phase sample was most representative of the conditions actually present in the column. The equilibrium data, however, was based upon the aqueous acid-thorium concentrations; therefore, for the organic continuous case, the profile sample values must be converted (by material balance calculation) to the corresponding aqueous values to be useable. With the exception of the feed point values, the actual and calculated aqueous thorium and acid values were, in general, in fair agreement (Table 7.6).

7.3 HETS Values for Thorium Extraction

HETS values for thorium extraction were calculated for various increments of the extraction section of sieve and nozzle plate columns, using the above procedure (Table 7.7). The most representative values were assumed to be those calculated for the longest possible length of the extraction section for which reliable analytical results were available (Table 7.8) and in general, were those calculated for the entire extraction section plus the bottom disengaging section. Incremental HETS profiles (Figure 7.4, 7.5 and 7.6) show that the most representative values were approximately equal to the average of the incremental HETS values.

The HETS value for aqueous-continuous operation of the sieve plate column was 2.1 ft for both salting acid to feed ratios tested. The HETS

¹J. W. Codding, W. O. Haas, Jr., and F. K. Heumann, "Tributyl Phosphate-Hydrocarbon Systems," I. and E. C., p. 145-152, Vol. 50. No. 2, February 1958.

³Private communication with R. H. Rainey, Oak Ridge National Laboratory.

UNCLASSIFIED
ORNL-LR-DWG 51329

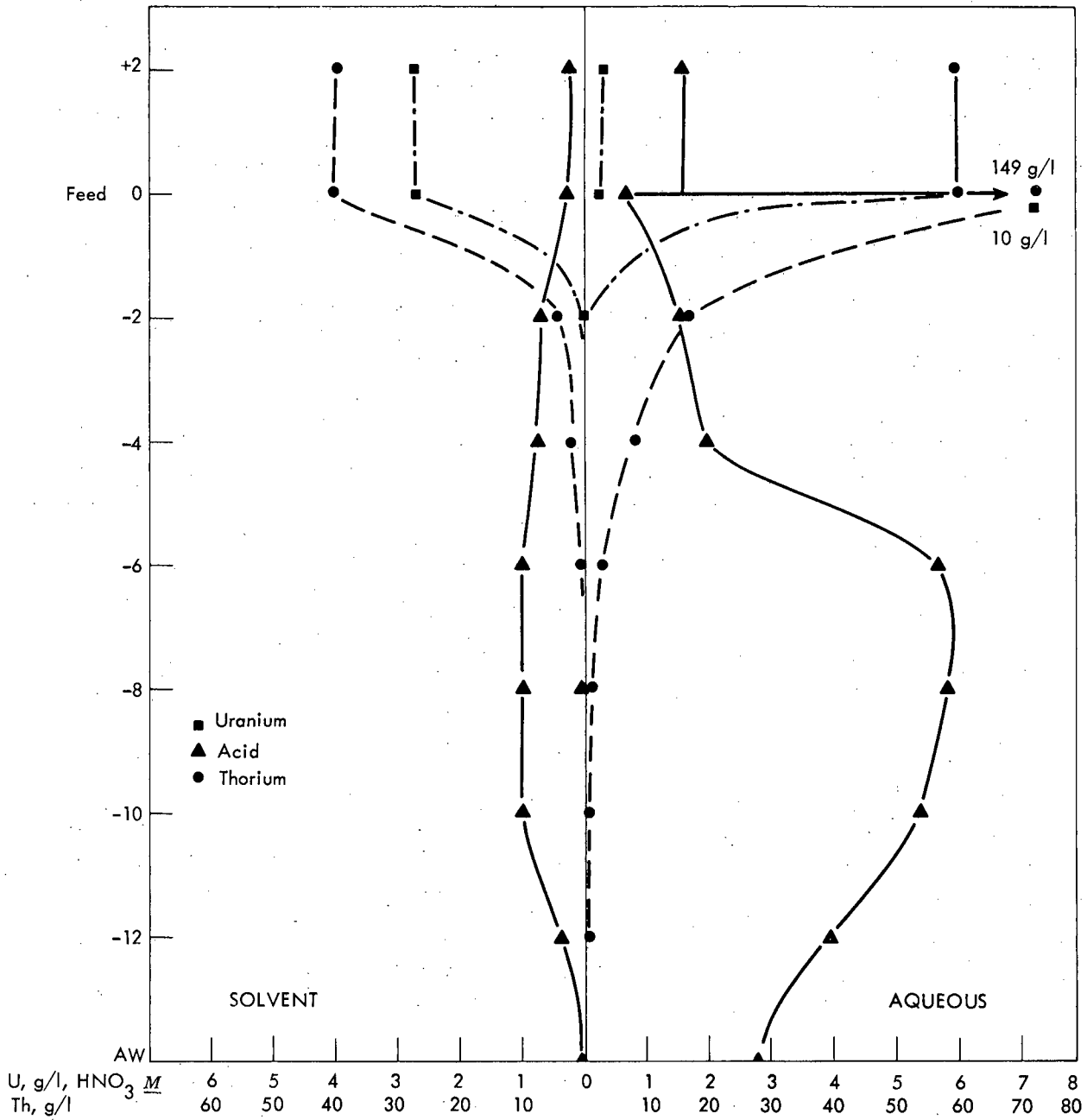


Fig. 7.2. Acid uranium + thorium concentration profile, AT-14.

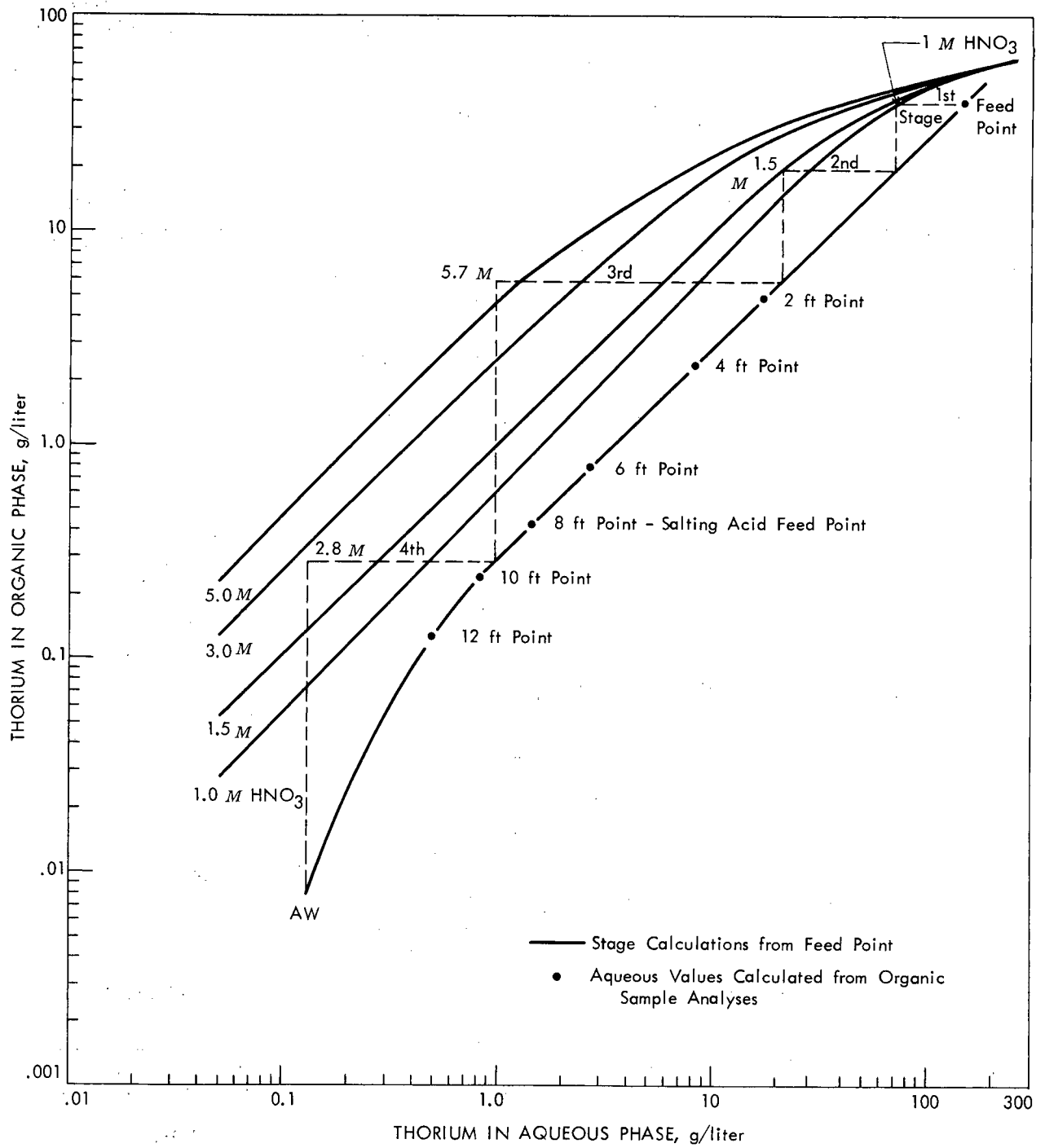


Fig. 7.3. McCabe-Thiele diagram, Run AT-14.

Table 7.6. Comparison of Calculated¹ and Actual Aqueous Thorium and H+ Concentrations

Location of Sample Points feet from feed point	AT-14				ATP-2				ATP-8				AT-17			
	Calc. ¹		Actual		Calc. ¹		Actual		Calc. ¹		Actual		Calc. ¹		Actual	
	Th g/l	H+ M	Th g/l	H+ M												
+2	59.6	1.6	59.4	1.5	68.0	1.9	53.0	2.0	116.0	1.7	-	-	63.2	1.9	72.9	1.9
Feed Point	149.0	0.7	63.0	1.5	158.0	0.9	60.6	1.7	181.0	0.8	-	-	155.0	0.8	91.7	1.6
-2	17.4	1.5	13.1	2.2	20.5	1.2	10.3	2.1	152.0	1.3	164.0	1.0	60.8	1.4	50.8	1.9
-4	8.2	2.0	5.53	2.9	5.91	1.5	4.46	2.6	48.7	2.0	-	-	15.2	2.1	12.6	2.6
-6	2.67	5.8	2.98	3.1	2.65	2.7	1.92	3.8	9.09	3.9	8.64	2.8	11.2	5.2	7.18	3.0
-8	1.42	5.8	1.05	5.7	0.78	6.3	0.75	5.6	3.73	4.1	-	-	-	-	-	-
-9	-	-	-	-	-	-	-	-	-	-	-	-	3.64	5.1	3.08	4.5
-10	0.82	5.6	0.36	5.2	0.20	6.1	0.45	3.3	0.60	3.8	-	-	-	-	-	-
-12	0.48	4.0	0.17	3.50	0.07	4.1	-	-	0.48	2.5	1.12	2.0	2.15	3.8	1.96	3.4

¹Calculated by material balance from organic samples.

Table 7.7. HETS (H) Values for Thorium Extraction

Run No.	Cont. Phase	Ratio Solting Acid Feed	Location of Section of Column Used in Calculations																													
			FP/-1	FP/-3	FP/-5	FP/-6	FP/-8	FP/-10	FP/-13	FP/bot.	-1/-3	-1/-5	-1/-6	-1/-8	-1/-10	-1/-13	-3/-5	-3/-6	-3/-8	-3/-10	-3/-13	-5/-6	-5/-8	-5/-10	-5/-13	-6/-8	-6/-10	-6/-13	-8/-10	-8/-13	-10/-13	
Sieve plate column: 0.125-in.-dia holes, 23% free area																																
AT-2	Aq.	0.5	0.83	1.3	1.7	1.9	2.1		3.1	3.0	1.7	2.1	2.5		4.0	2.5	3.3			5.0	2.3				5.3	2.3		5.3		6.6		
AT-3	Aq.	0.3	0.90	1.5	1.7	1.9	2.1			3.3	2.2	2.1	2.5	2.6			2.2	2.6	2.8			2.2	3.5			3.2						
AT-23	Org.	0.5	2.0	1.8	2.1	2.3	2.8	3.3	4.2	4.0	1.5	2.1	2.5	2.7	3.3	4.5	2.7	3.3	3.9	4.5	5.6	2.6	3.9	5.7	8.3	3.3	5.4	8.0	5.4	7.6	7.0 ¹	
Large nozzle plate column: 0.188-in.-dia holes, 23% free area																																
			FP/-2	FP/-4	FP/-6	FP/-9	FP/-12	FP/bot.	-2/-4	-2/-6	-2/-9	-2/-12	-4/-6	-4/-9	-4/-12	-6/-9	-6/-12	-9/-12														
AT-17	Org.	0.5	1.2	1.5	2.1	3.0	3.7	3.7	2.4	4.1	4.7	5.7	4.2	6.2	8.6	5.1	7.2	6.7 ²														
			1.4	1.6	2.3	3.0	4.0	4.0	2.0	3.2	3.9	5.3	7.4	6.3	7.9	4.3	6.7	7.1 ¹														
Small nozzle plate column: 0.125-in.-dia holes, 10% free area																																
			FP/-2	FP/-4	FP/-6	FP/-8	FP/-10	FP/-12	FP/bot.	-2/-4	-2/-6	-2/-8	-2/-10	-2/-12	-4/-6	-4/-8	-4/-10	-4/-12	-6/-8	-6/-10	-6/-12	-8/-10	-8/-12	-10/-12								
AT-14	Org.	0.5	0.9	1.5	2.1	2.3	2.6	3.0	3.0	3.1	4.7	5.0	4.5	5.2	4.0	4.4	4.6	4.6	2.9	4.2	4.4	2.9	7.5	3.5 ²								
			0.9	1.5	2.1	2.7	3.2	3.4	3.0	3.6	4.5	6.2	8.0	6.7	2.9	4.3	6.0	5.3	3.9	5.1	6.4	4.0	5.0	4.0 ¹								
ATP-2	Org.	0.5	0.8	1.4	2.0	2.2	2.7	3.0	2.5	3.2	4.4	4.9	4.9	5.1	3.2	4.4	5.5	4.6	3.1	4.8	2.2	4.5	4.5	3.0 ²								
			0.8	1.2	1.6	2.0	2.2	2.4	2.4	2.0	2.6	3.2	3.5	3.5	3.7	2.2	5.6	4.4	2.8	4.3	4.0	2.4	3.7	2.8 ¹								
ATP-8	Org.	0.3								0.9	1.1	1.6	1.7	2.1	1.4	2.2	3.5	4.4	3.0	2.6	3.5	2.1	4.0	5.1 ^{1,3}								

Pulse Frequency = 50 cpm; Pulse Amplitude = 1 in.

¹HETS values based on aqueous values calculated from organic sample analyses.

²HETS values based on aqueous sample analyses.

³Flow ratios differ from preceding runs.

Table 7.8. Most Representative HETS Values for Thorium Extraction

Run No.	Column Cartridge	Continuous Phase	% of Flooding Rate	Most Representative HETS Values, ft	
				Based on Aqueous Samples	Based on Organic Samples
AT-2	Sieve	Aqueous	55	2.1	-
AT-3	Sieve	Aqueous	55	2.1	-
AT-23	Sieve	Organic	33	-	4.0
AT-17	Large nozzle	Organic	< 80	3.7	4.0
AT-14	Small nozzle	Organic	78	3.0	3.0
ATP-2	Small nozzle	Organic	46	2.5	2.4
ATP-8	Small nozzle	Organic	46	-	2.1

value for sieve plate column operated organic continuous was 4.0 ft.

HETS values for organic-continuous operation of the nozzle plate columns were determined using both the aqueous sample analyses and aqueous thorium and acid concentrations calculated by material balance from the organic sample analyses. In general, these values differed by 10% or less (Table 7.6), indicating that aqueous sample analyses were quite representative of the conditions actually present in the column and, concomitantly, HETS values determined from them were also valid. HETS values for thorium extraction in the large nozzle plate column were 3.7 ft based on aqueous samples and 4.0 ft based on organic samples. The HETS values obtained with the small nozzle plates were 3.0 ft (either case) for 970 gal sq ft⁻¹ hr⁻¹ flow rate and 2.5 ft (aqueous samples) and 2.4 ft (organic samples) for 570 gal sq ft⁻¹ hr⁻¹ flow rate.

Run ATP-8 was made using greater feed flow rate than in the preceding tests. Although the column achieved steady state conditions which gave excellent thorium extraction, it was operating very close to "pinching" at the feed point. The HETS values for 2.1 ft (Table 7.8) was calculated for the length of column starting 2 ft below the feed point to avoid the uncertainty involved by operating close to the pinch point.

UNCLASSIFIED
ORNL-LR-DWG 51331

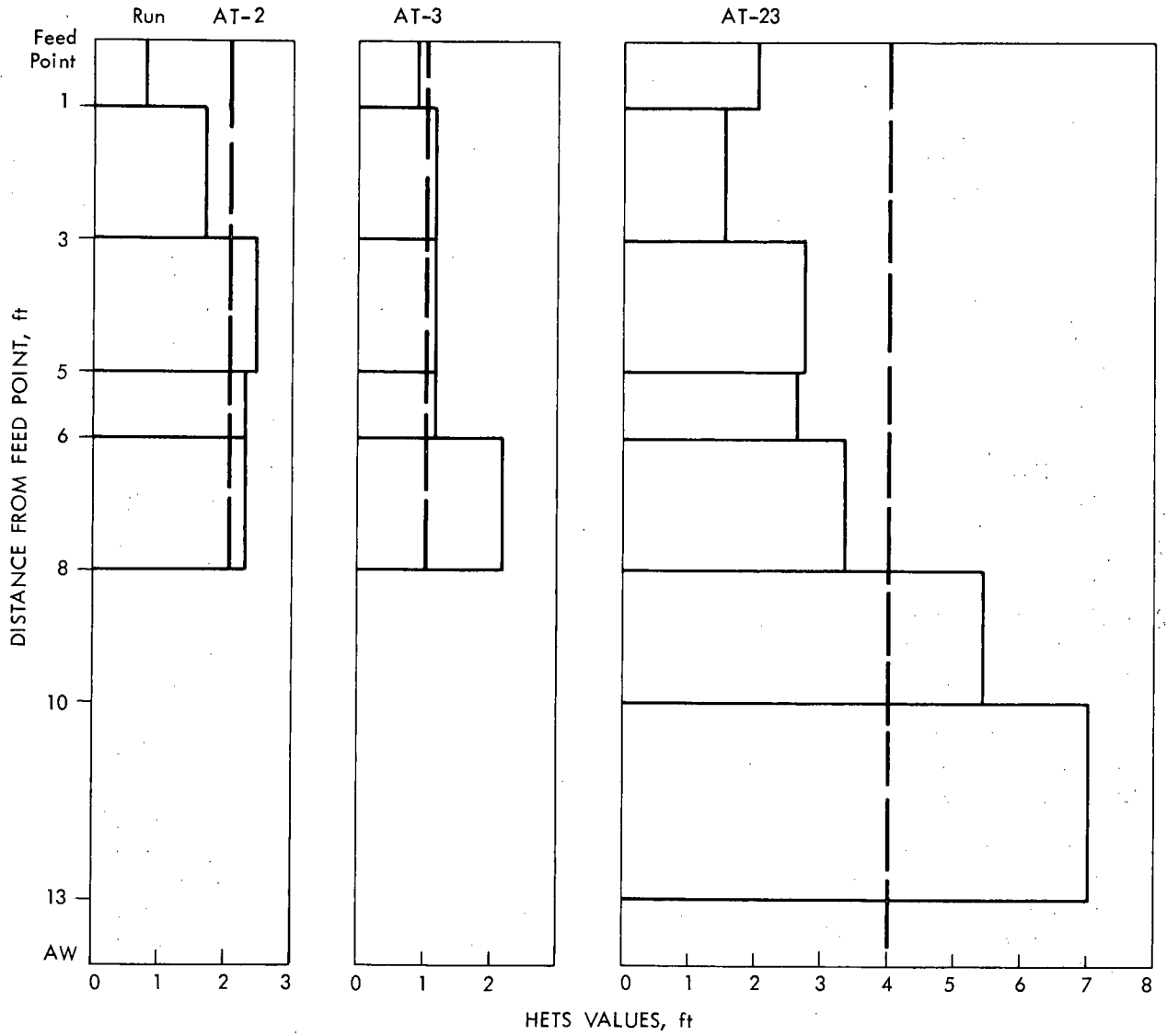


Fig. 7.4. Incremental HETS profile.

UNCLASSIFIED
ORNL-LR-DWG 51332

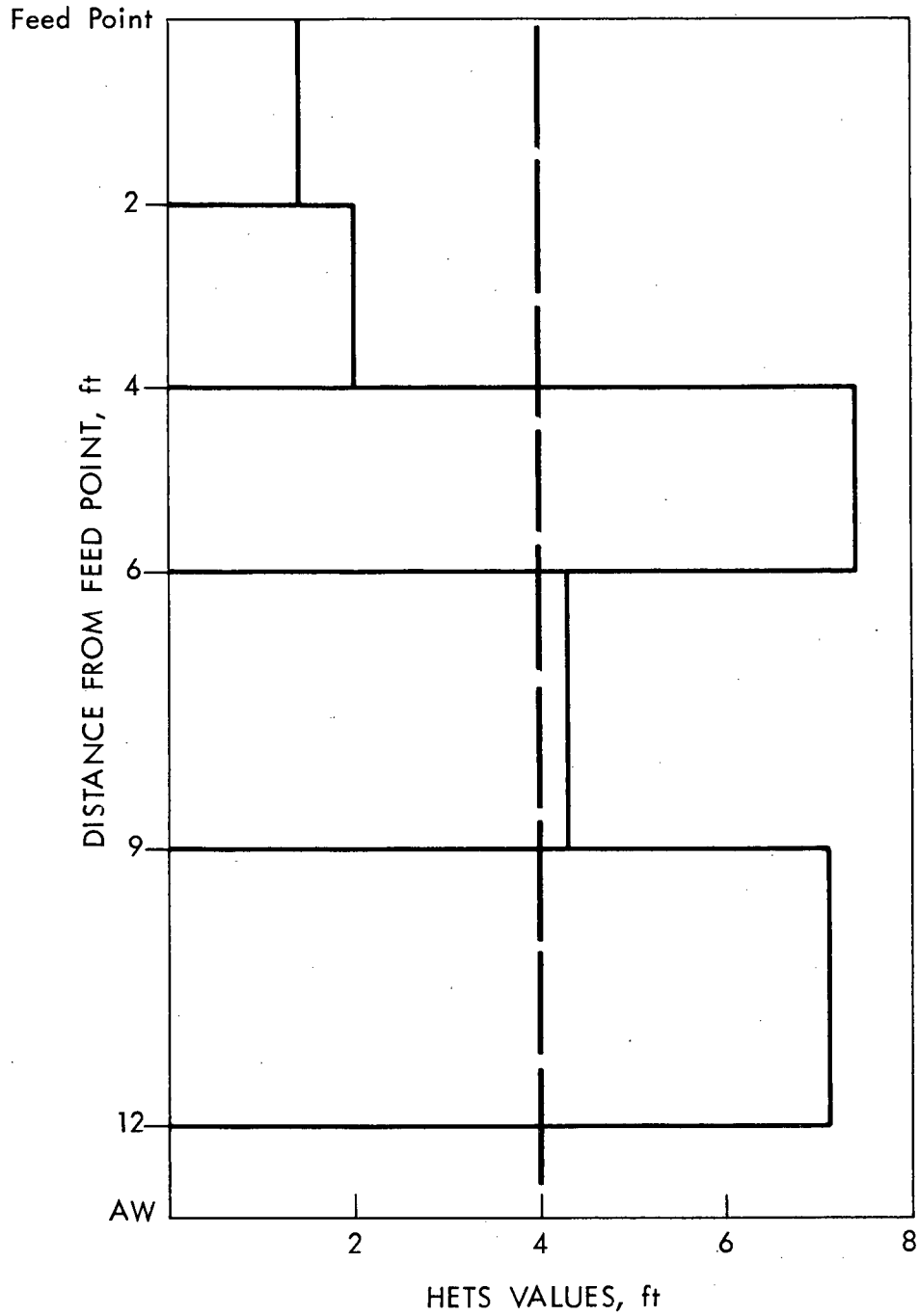


Fig. 7.5. Incremental HETS profiles, Run AT-17.

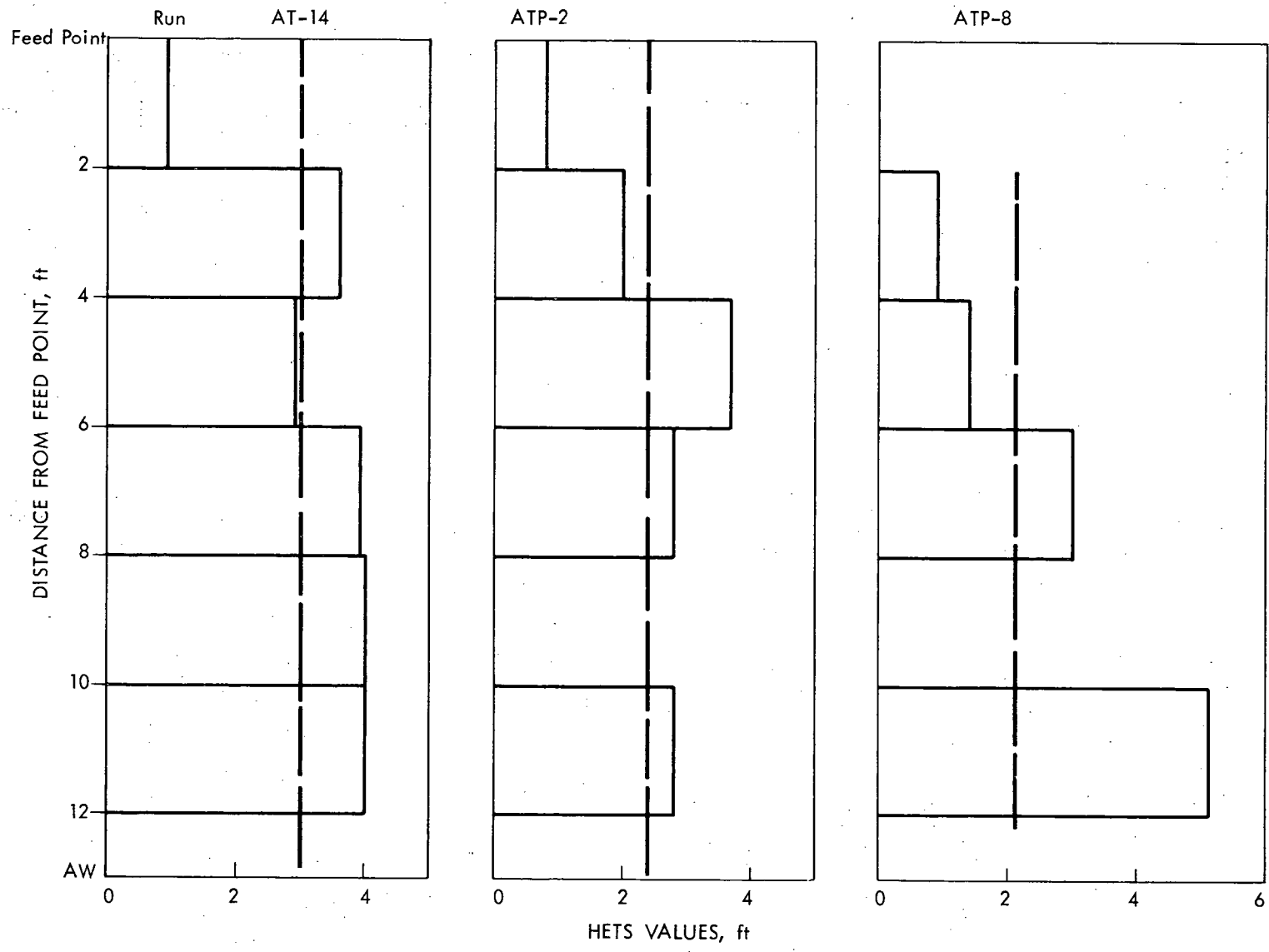


Fig. 7.6. Incremental HETS profile.

8.0 VOLATILITY

R. W. Horton

8.1 Volatility Studies on Complexes of Fission Product Fluorides with NaF - F. R. Groves, Jr.

A program for study of the absorption of volatile fission product fluorides by NaF has been started. As a working hypothesis we are assuming that this absorption process involves chemical complex formation between NaF and the volatile fluoride. The specific object of the experimental program is to measure the dissociation pressures of these complexes as a function of temperature. The volatile fluorides of molybdenum, niobium, ruthenium, and chromium have been selected for exploratory study. MoF_6 (b. pt. 35°C) will be studied first because it is easy to prepare and can be handled readily as a gas at moderate temperatures.

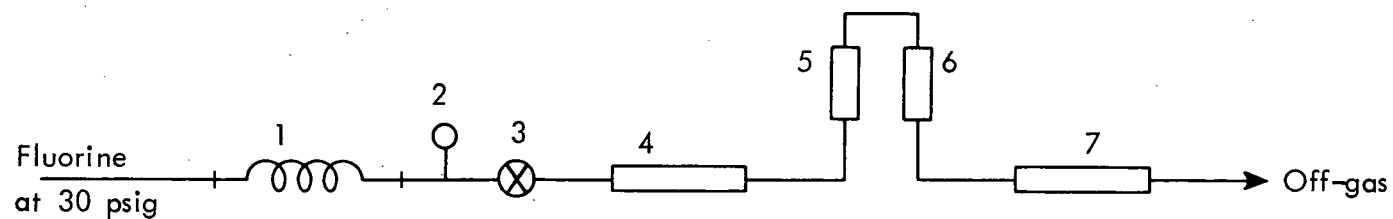
Preparation of the Volatile Fluorides. It was decided to prepare the fission product fluorides by direct reaction of the elements. The fluorides are volatile and quite sensitive to moisture. Since the fluoride complex with NaF is the compound to be studied, it was thought best to prepare the complex immediately without isolating and purifying the fluoride itself. The procedure for preparing MoF_6 will be described because this material is to be studied first. The preparation of other fluorides will be the same except for temperatures required.

The train of apparatus shown in Figure 8.1 was constructed. Fluorine from a tank at 30 psig is metered through a capillary to a fluorinator vessel where it contacts molybdenum powder. MoF_6 formed in the fluorinator is swept by the fluorine stream through two absorbers which contain 1/8-in. NaF pellets. The MoF_6 reacts with the contents of the absorber forming the complex $(\text{NaF})_x \cdot (\text{MoF}_6)_y$. The fluorine stream passes on to a chemical trap where it is absorbed by soda lime.

The vessels in the fluorination system were connected together with 1/4-in. copper tubing. The fluorinator and absorber vessels were identical and were made from 3/4-in. copper tubing. The dimensions of these vessels are shown in Figure 8.2. The metals to be fluorinated and the NaF pellets in the absorbers were held in Monel carrying tubes which fit inside the fluorinator and absorbers. These tubes were closed at the lower end by Monel screen and could be removed easily for accurate weighing on the analytical balance. The tubes were threaded at their upper ends and were screwed into the closures of the absorbers which were tapped to receive them. Figure 8.3 shows the dimensions of the carrying tubes. They were made from 3/8-in. Monel pipe turned down to fit inside the absorbers. The carrying tubes were made in two sizes, 6-in. and 12-in. overall length. The 6-in. tubes weighed about 50 g empty; the 12-in. tubes weighed about 100 g.

The absorber vessels were wound with 36 ft of 20 gauge Nichrome resistance wire and were then wrapped with approximately two layers of asbestos tape. This arrangement provided electrical heating capacity of about 500 watts at 110 volts. All connecting tubing was wound with Nichrome resistance wire and asbestos tape to permit heating. The fluorinator was heated by a 2200 watt (110 volt) "clam shell" heater. All heaters were manually controlled by Variacs.

UNCLASSIFIED
ORNL-LR-DWG 51334



- 1 Type 347 stainless steel capillary, 2 ft long, 20 mil i.d., 20 mil wall thickness.
- 2 Gage, brass trim, 0 - 30 psig.
- 3 Monel valve, Hoke.
- 4 Fluorinator vessel, copper.
- 5 Absorber, copper.
- 6 Absorber, copper.
- 7 Chemical trap, soda lime.

Fig. 8.1. Apparatus for preparation of fission product fluorides.

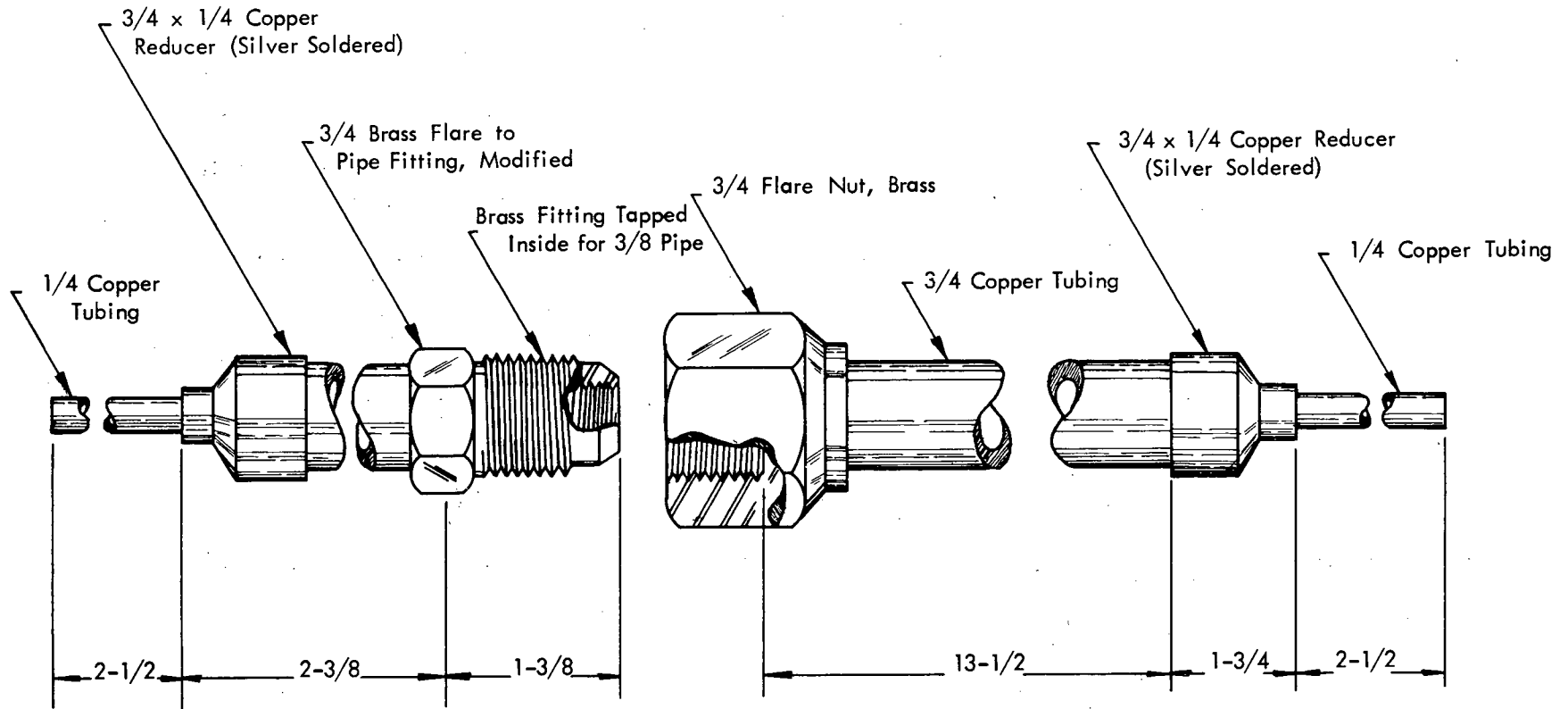


Fig. 8.2. Fluorinator or absorber vessel.

UNCLASSIFIED
ORNL-LR-DWG 51340

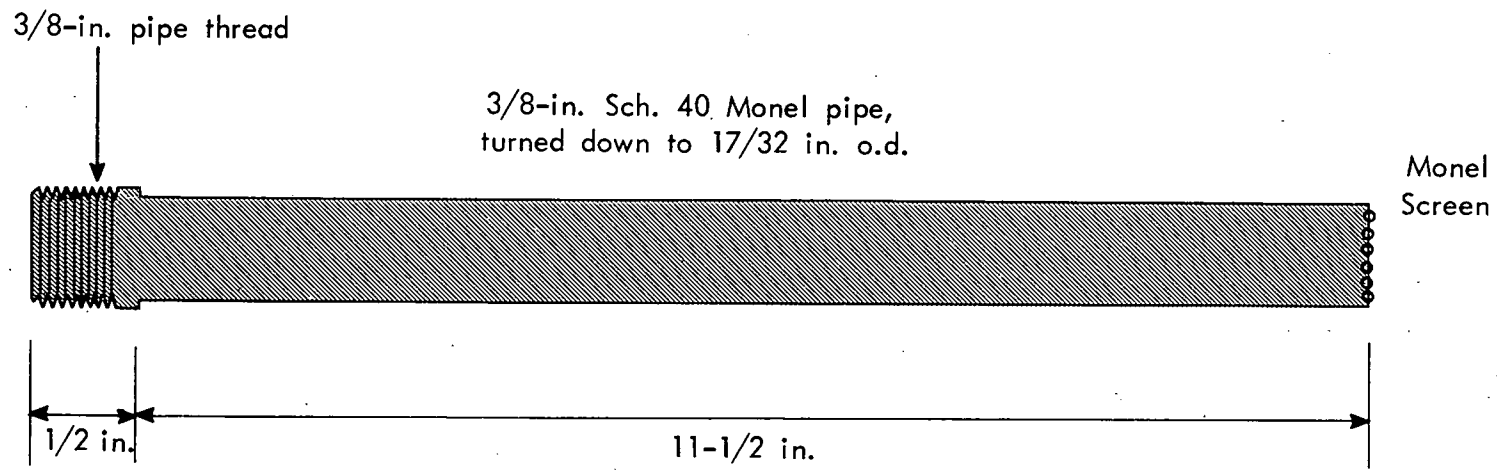


Fig. 8.3. Monel carrying tube, 12 in.

Preparation of MoF₆. A first attempt to prepare MoF₆ was made by passing fluorine (about 800 cc/min) over 5.8 g of powdered molybdenum (99.8%, 200 mesh) for 1/2 hr. During the treatment with fluorine the temperature of the fluorinator was raised from 30° to 125°C by means of an electrical heater. After exposure to fluorine the tube containing the molybdenum powder showed a loss in weight of 0.064 g. No significant weight change was detected in the absorbers.

It was decided to repeat the preparation with a higher fluorinator temperature and a longer period of exposure to fluorine.

Apparatus for Measurement of Dissociation Pressure. The method proposed for measurement of dissociation pressure is the dynamic method, which has often been used for vapor pressure measurements. The flow system for this experimental method is shown in Figure 8.4.

The operation of the system is as follows:

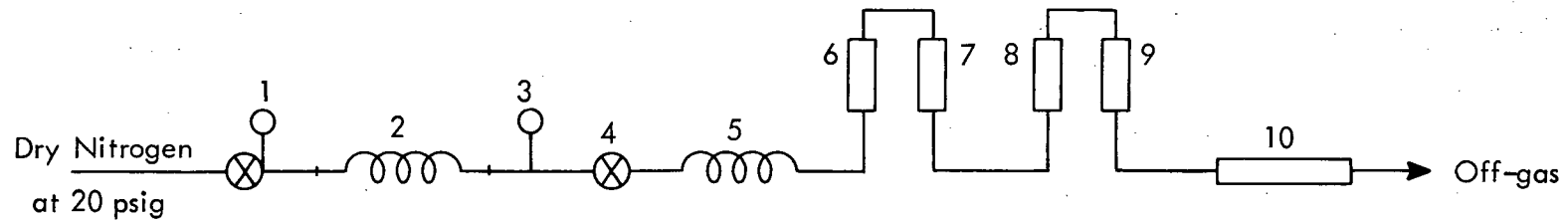
Dry nitrogen is metered through the capillary to the presaturator and saturator which contain the complex, e.g., (NaF)_x · (MoF₆)_y whose dissociation pressure is to be measured. These vessels are held at some constant elevated temperature at which the complex has an appreciable vapor pressure. The nitrogen emerges saturated with the volatile fluoride—the partial pressure of fluoride in the nitrogen stream equals the dissociation pressure of the fluoride-NaF complex. The mixture of nitrogen and volatile fluoride passes to the absorbers which contain NaF pellets held at a temperature low enough that the fluoride-NaF complex has negligible dissociation pressure. The volatile fluoride is absorbed out completely, forming the complex. The nitrogen stream passes to the off-gas system. The loss in weight of the saturators gives the mols, m, of volatile fluoride removed by the metered quantity, G mols, of nitrogen passed through the system. The gain in weight of the absorbers gives a check on the quantity m. The total pressure P at the saturator outlet is measured by means of a manometer. Then, assuming ideal gas behavior, the dissociation pressure of the complex can be calculated from the following formula

$$p = \left(\frac{m}{G + m} \right) P$$

where m, G, P are defined above and p is the dissociation pressure of the complex at the saturator temperature.

The above train of equipment has been constructed. The absorber and saturator vessels were made identical to the vessels described above for the fluorination apparatus. The preheater was made from 3 ft of 1/4-in. copper tubing wound into a 3-in.-dia coil. The preheater was wrapped with 36 ft of 20 gauge Nichrome resistance wire plus asbestos tape to provide 500 watts (110 volts) electrical heating capacity. The connecting tubing was 1/4-in. copper wound with Nichrome resistance wire and asbestos tape. The presaturator and saturator were heated by means of "clam shell" heaters (2200 watts, 110 volts).

UNCLASSIFIED
ORNL-LR-DWG 51335



- 1 Pressure regulator, 0-30 psig.
- 2 Type 347 stainless steel capillary, 5 ft long, 20 mil i.d., 20 mil wall thickness.
- 3 Pressure gage, 0-30 psig.
- 4 Valve, monel, Hoke.
- 5 Preheater.
- 6 Presaturator.
- 7 Saturator.
- 8,9 Absorbers.
- 10 Chemical trap, soda lime.

Fig. 8.4. Apparatus for dynamic method of dissociation pressure measurement.

The above system will be tested after MoF_6 and NbF_5 have been prepared. Two sources of difficulty are quickly seen in the proposed method:

1. Will the exposure time of the nitrogen stream to the complex in the saturators be sufficient to allow equilibrium to be attained? That is, will the nitrogen stream be saturated when it leaves the saturator? If the rate of transfer of volatile fluoride from complex to nitrogen stream is slow, then equilibrium won't be reached. If equilibrium can't be attained, the measurements will provide only a lower limit for the dissociation pressure of the complex. In any case the data should be useful as an indication of the rate of desorption of volatile fluorides from NaF beds, especially for comparison of desorption rates of different fluorides.

2. Will the NaF pellets in the absorbers remove all the volatile fluoride from the nitrogen stream as it passes through? If not, some other sort of absorber, perhaps a cold trap, might be tried. Actually the gain in weight of the absorbers just provides a check on the loss in weight of the saturators so the absorbers can be omitted if desired. In any case they will provide useful information on the rate of absorption of volatile fluorides on NaF beds.

The above two difficulties will be dealt with during the preliminary testing of the equipment for measuring dissociation pressure.

9.0 WASTE PROCESSING

J. C. Suddath

Study of pot calcination for high level liquid waste disposal was continued, with emphasis on providing engineering design data for full scale plant design. One calcination run, R-31, was made with simulated Purex waste containing stable ruthenium. An apparatus is being built for studying the growth of soluble aerosols in a wetted wall tower.

9.1 Purex Calcination Run R-31 - C. W. Hancher

The major purpose of test R-31 was to determine the effect of diameter of the calciner vessel on solid deposition rate. The mathematical model predicted that feed rate should be independent of vessel diameter (June 1960 Unit Operations monthly progress report). Ruthenium as RuCl_3 was added to the feed mixture (0.0017 M or 0.02 g/liter as Ru) to attempt to measure its distribution between solid and condensate.

The feed for test R-31 was synthetic Purex feed (40 gal/ton)(Table 9.1). The diameter of the calciner vessel was 7-in. The vessel was 84-in. long and had six sets of 4 thermocouples similar to calcination vessels for runs 29 and 30 (Figure 9.1). Calcium oxide was added (0.62 M) to the feed mixture to decrease sulfate vaporization. A bleeding dip-tube liquid level probe was used to maintain the liquid level at 72-in. from the bottom of calciner vessel, as in runs 29 and 30.

The waste processing rate averaged over the feeding period for test 31 was 25.6 liters per hour (Table 9.2). The calcination time after the feeding period was five hours. Upon inspection the vessel was found to be only about 90% full, having a void volume down the center about 3-in. in diameter and 30-in. long. In runs 29 and 30, carried out in 8-in. and 6-in. dia vessels, the average feed rate to fill 90% of the vessel volumes was 20 liters/hr for both runs. The average feed rate in run 31 was higher due to overflow of the feed solution into the condensate, which was probably caused by excessive foaming. Samples of the condensate were found to be very high in calcium and sodium, but not proportionally high in iron (Table 9.1). The condensate contained a precipitate which the sampling system was not equipped to handle; therefore, condensate samples were probably not representative.

Since 85% of the iron fed to the vessel was found in the calcined solids, while less than half of the sodium and calcium were, preferential carry-over of the sodium and calcium by the foam must have occurred. The unusual solid composition probably accounts for the low solid density of 1.2 g/cc, compared with 1.5 to 1.6 g/cc in previous runs.

Ruthenium was added (0.0017 M) to simulate radioactive ruthenium, and it was hoped that a distribution between cake and condensate could be determined. Only 16% of ruthenium in the feed was found in solid sample; however, it is very difficult to get a representative sample of the solid. The condensate sampling system was not equipped to handle solids, therefore

Table 9.1. Material Balance for Test R-31

		Ca	Na	Fe	NO ₃	SO ₄	Ru
Feed	Molar	0.62	1.23	0.43	5.9	1.4	0.002
	g mol	155	333	108	1480	370	0.47
	%	100	100	100	100	100	100
Cond.	Molar	0.05	0.1	0.03	4.9	0.1	0.0005
	g mol	12	23	7	1200	46	0.12
	%	8	8	4	81	12	25
Solid	wt %*	3	7	11	60 ppm	55	0.02
	g mol	38	150	91	-	290	0.08
	%	25	45	85	-	78	16
Unaccounted for	%	67**	47**	11	19	10	** 59***

* Only 76 wt %, rest oxide + water.

** Non-representative condensate sample.

*** Analytical difficulty using solids for Ru.

Table 9.2. Calciner Test R-31 Results

Purex Waste (40 gal/ton)

Pot dia - 7-in.

Average feed rate - 25.6 liter/hr (307 liter/12 hrs)

Calcining Time - 5 hrs

Bulk density - 1.2 g/cc (including void vol.)

Cr⁵¹ tracer injected but solid was broken from side wall so analysis was impossible

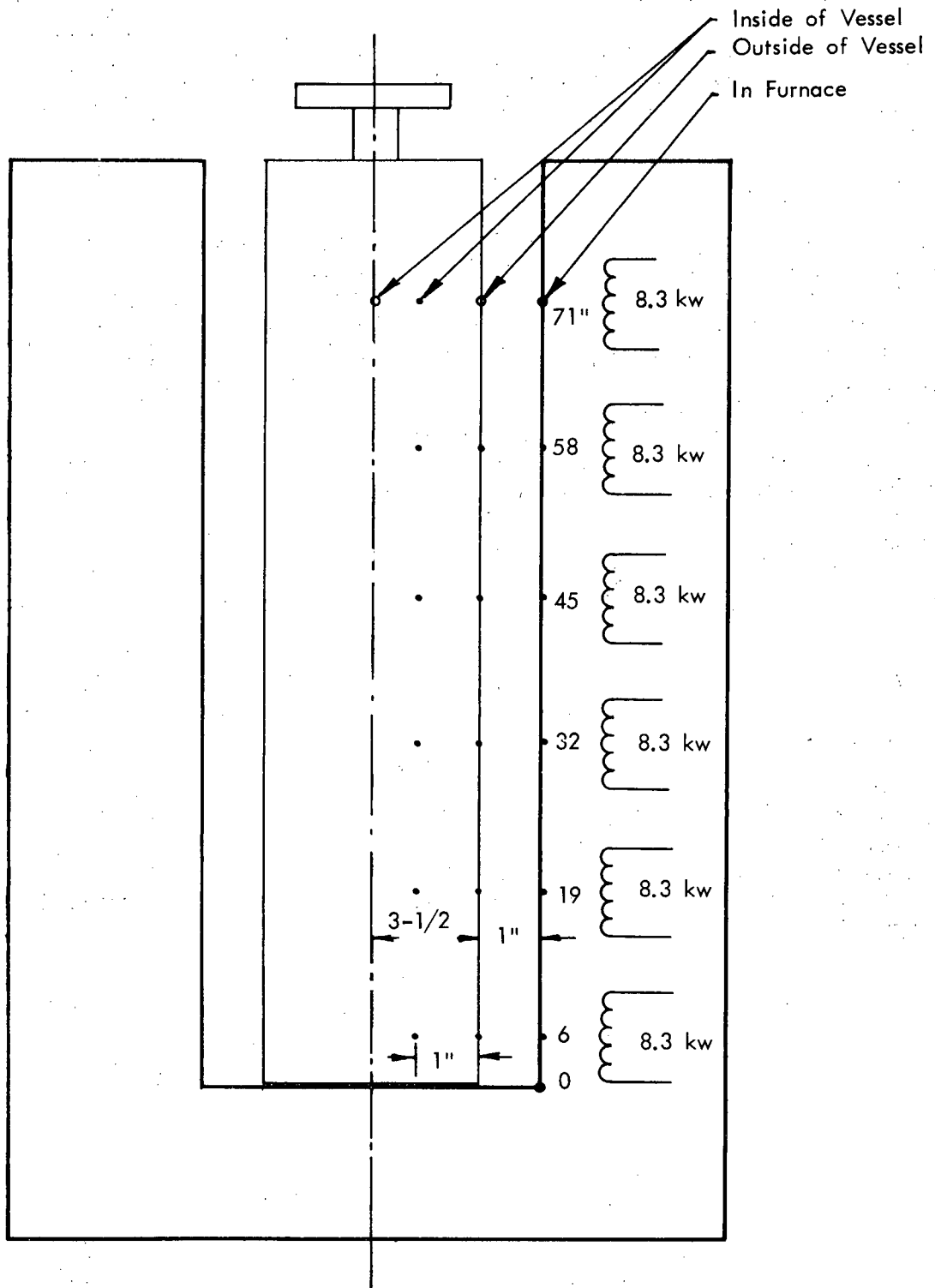


Fig. 9.1. Thermocouple positions for Test R-31.

condensate samples may be low because not all of the solids in the condensate were sampled. The composite condensate sample showed only 25% of the ruthenium which leaves 59% unaccounted for. The condensate sampling procedure is being changed to handle solids.

The off-gas rate was not measured because of malfunction of the jet scrubber, which maintained a 1 psig negative pressure on the system. The wet-test meter had to be by-passed because it could not operate in NO-NO₂ fumes.

9.2 Calciner Off-Gas Treatment - J. J. Perona

In previous experiments the attenuation of a soluble aerosol in a packed tower was shown to be greatly enhanced by the presence of steam in the vapor phase. Decontamination factors for an air stream bearing 10 to 15 μ diameter aerosols containing a radioactive tracer were less than 10 in an ambient temperature packed scrubber and greater than 5×10^3 when the liquid phase was boiled and refluxed (CF 60-3-61, p. 62 and CF 60-4-37). The mechanism of attenuation is believed to involve growth of the aerosol due to the difference in vapor pressures between the solute-containing aerosols and the bulk gas phase. Sufficient growth would result in attenuation of the aerosol by inertial effects as the gas phase rises through the tortuous passages of the wetted packing.

In order to study separately the phenomenon of aerosol growth, a wetted wall tower is being constructed with provisions for sampling an aerosol stream before and after passage through the tower. A flowsheet of the apparatus is given in Figure 9.2. Three 1000 watt heaters were installed in the water reservoir, which is a 25 liter battery jar. Experiments with water phase temperature in excess of 90°C should be possible.

The spinning disc aerosol generator was made by constructing a housing, with air inlets and outlets and a solution feed line, for a Bellows grinder (model CR-125A) which spins a 1-in. dia disc at speeds up to 100,000 rpm (Figure 9.3). In tests with 94 psig air and feeding 2% NaCl solution at a rate of 0.2 cc/min, 94.9% of the particles were between 1.5 and 5 μ in dia (Table 9.3).

Table 9.3. Particle Size Distribution of NaCl Aerosol

<u>Size Range</u> microns	<u>Percentage</u>
<1.5	21.0
1.5-2.7	47.9
2.7-5.0	47.0
>5.0	3.1

A pressure difference of 0.4 in H₂O was maintained between the upper and lower chambers of the generator to remove the small satellite particles.

The growth of the aerosol particles will be studied as a function of water temperature and residence time.

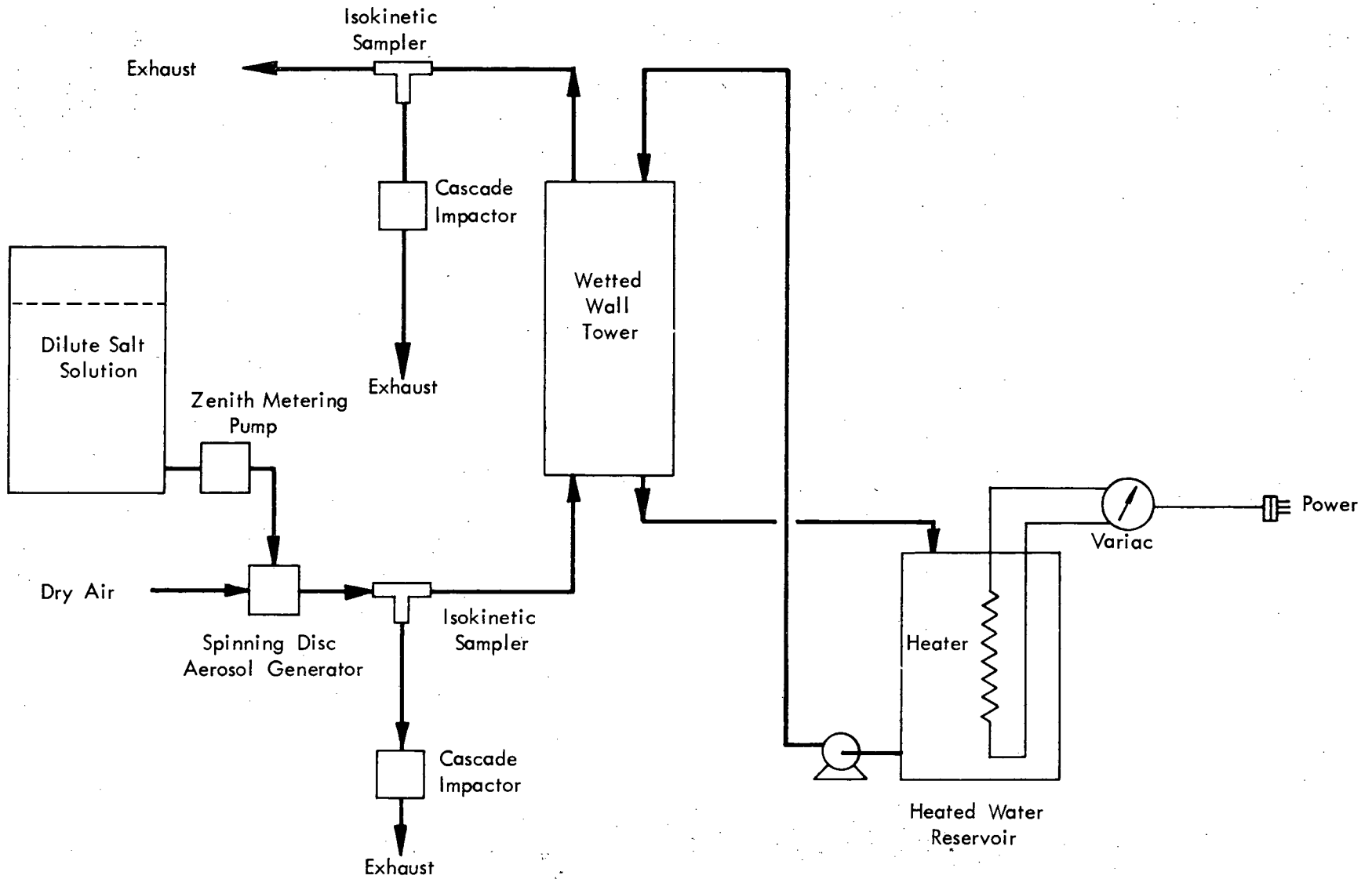


Fig. 9.2. Flowsheet of apparatus for aerosol growth studies.

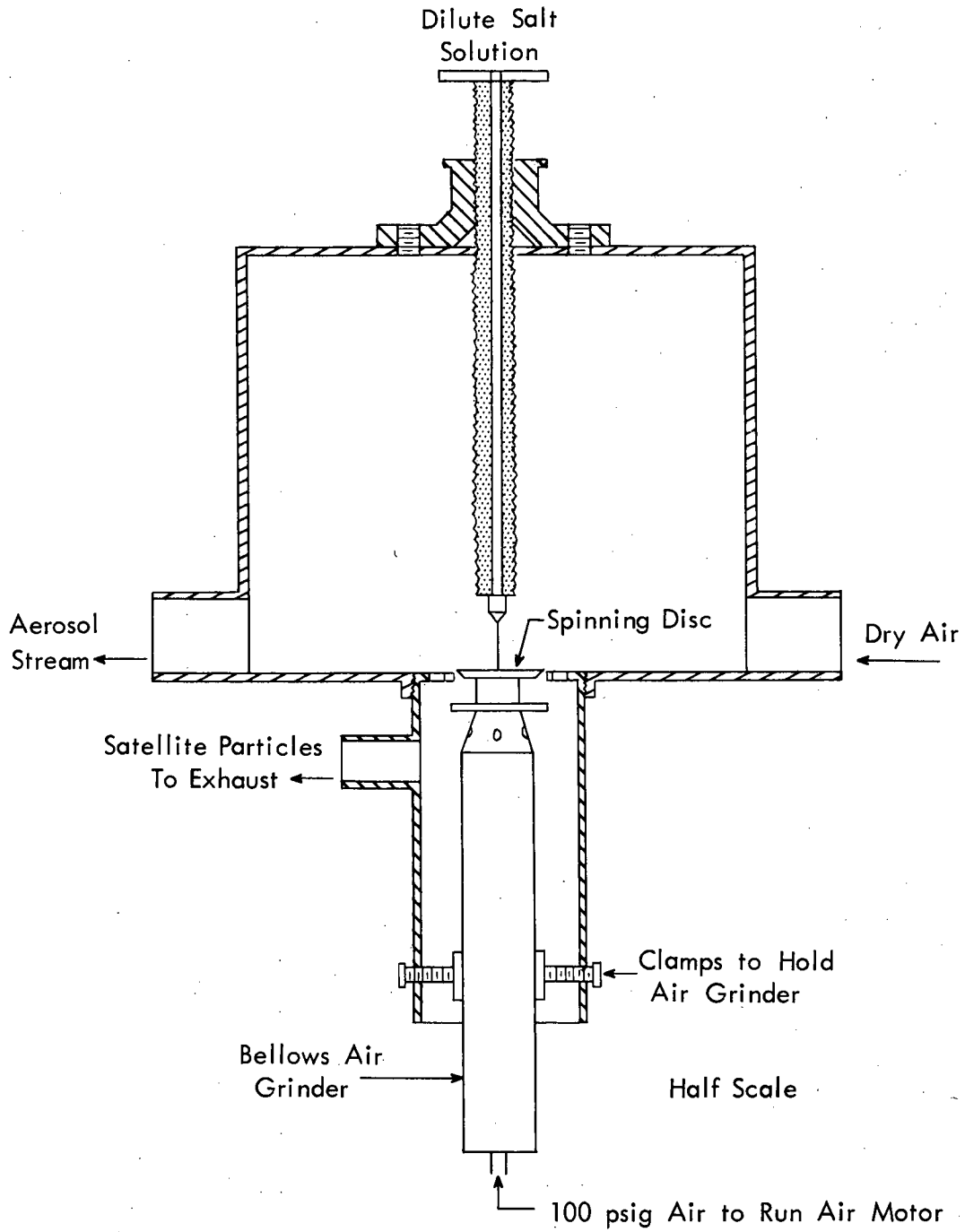


Fig. 9.3. Assembly of spinning disc aerosol generator.

DISTRIBUTION

- | | |
|---|--|
| 1. E. L. Anderson (AEC Washington) | 52. W. H. Lewis |
| 2. F. P. Baranowski (AEC Washington) | 53. J. A. Lieberman (AEC Washington) |
| 3. W. G. Belter (AEC Washington) | 54. R. B. Lindauer |
| 4. R. E. Blanco | 55. A. P. Litman |
| 5. J. O. Blomeke | 56. J. T. Long |
| 6-9. J. C. Bresee | 57. B. Manowitz (BNL) |
| 10. R. E. Brooksbank | 58. J. L. Matherne |
| 11. K. B. Brown | 59. J. A. McBride (ICPP) |
| 12. F. R. Bruce | 60. J. P. McBride |
| 13. L. P. Bupp (HAPO) | 61. W. T. McDuffee |
| 14. W. D. Burch | 62. R. A. McNees |
| 15. W. H. Carr | 63. R. P. Milford |
| 16. G. I. Cathers | 64. J. W. Morris (SRP) |
| 17. J. T. Christy (HOO) | 65. D. M. Paige (ICPP) |
| 18. W. E. Clark | 66. J. R. Parrott |
| 19. V. R. Cooper (HAPO) | 67. F. S. Patton, Jr. (Y-12) |
| 20. K. E. Cowser | 68. H. Pearlman (AI) |
| 21. F. E. Croxton (Goodyear Atomic Corp.) | 69. R. H. Rainey |
| 22. F. L. Culler, Jr. | 70. J. T. Roberts |
| 23. W. Davis, Jr. | 71. C. A. Rohrmann (HAPO) |
| 24. O. C. Dean | 72. O. T. Roth (AEC Washington) |
| 25. W. K. Eister | 73. A. D. Ryon |
| 26. D. E. Ferguson | 74. W. F. Schaffer |
| 27. L. M. Ferris | 75. C. H. Secoy |
| 28. R. J. Flanary | 76-78. E. M. Shank |
| 29. E. R. Gilliland (Consultant MIT) | 79. M. J. Skinner |
| 30. H. E. Goeller | 80. C. M. Slansky (ICPP) |
| 31. M. J. Googin (Y-12) | 81. S. H. Smiley (ORGDP) |
| 32. A. T. Gresky | 82. E. G. Struxness |
| 33. P. A. Haas | 83. J. C. Suddath |
| 34. M. K. Harmon (HAPO) | 84. J. A. Swartout |
| 35. F. E. Harrington | 85. R. J. Teitel (Dow Chemical Co., Midland Mich.) |
| 36. L. P. Hatch (BNL) | 86. F. M. Tench (Y-12) |
| 37. O. F. Hill (HAPO) | 87. V. R. Thayer (duPont, Wilmington, Del.) |
| 38. J. M. Holmes | 88. W. E. Unger |
| 39. R. W. Horton | 89. J. Vanderryn (AEC ORO) |
| 40. A. R. Irvine | 90. F. M. Warzel (ICPP) |
| 41. G. Jasny (Y-12) | 91. C. D. Watson |
| 42. H. F. Johnson | 92-121. M. E. Whatley |
| 43. W. H. Jordan | 122. G. C. Williams |
| 44. S. H. Jury | 123. R. H. Winget |
| 45. K. K. Kennedy (IDO) | 124. C. E. Winters |
| 46. L. J. King | 125. R. G. Wymer |
| 47. B. B. Klima | 126-127. Central Research Library |
| 48. E. Lamb | 128-131. Laboratory Records |
| 49. D. M. Lang (ORGDP) | 132. Laboratory Records (RC) |
| 50. S. Lawroski (ANL) | 133. Document Reference Section |
| 51. R. E. Leuze | |